



Advanced MHD models of anisotropy, flow and chaotic fields

M. J. Hole¹, M. Fitzgerald¹, G. Dennis¹, Zhisong Qu¹,
S. Hudson², R. L. Dewar¹, D. Terranova³, L. C. Appel⁴,
P. Franz³, G. von Nessi¹, B. Layden¹

[1] Australian National University, ACT 0200, Australia

[2] Princeton Plasma Physics Laboratory, New Jersey 08543, U.S.A.

[3] Consorzio RFX, Padua, Italy

[4] EURATOM/CCFE Fusion Assoc., Culham Science Centre, Abingdon, Oxon OX14 3DB, UK

International Congress on Plasma Physics

9-12 February, 2014

Funding Acknowledgement: Australian Research Council, DIISRTE

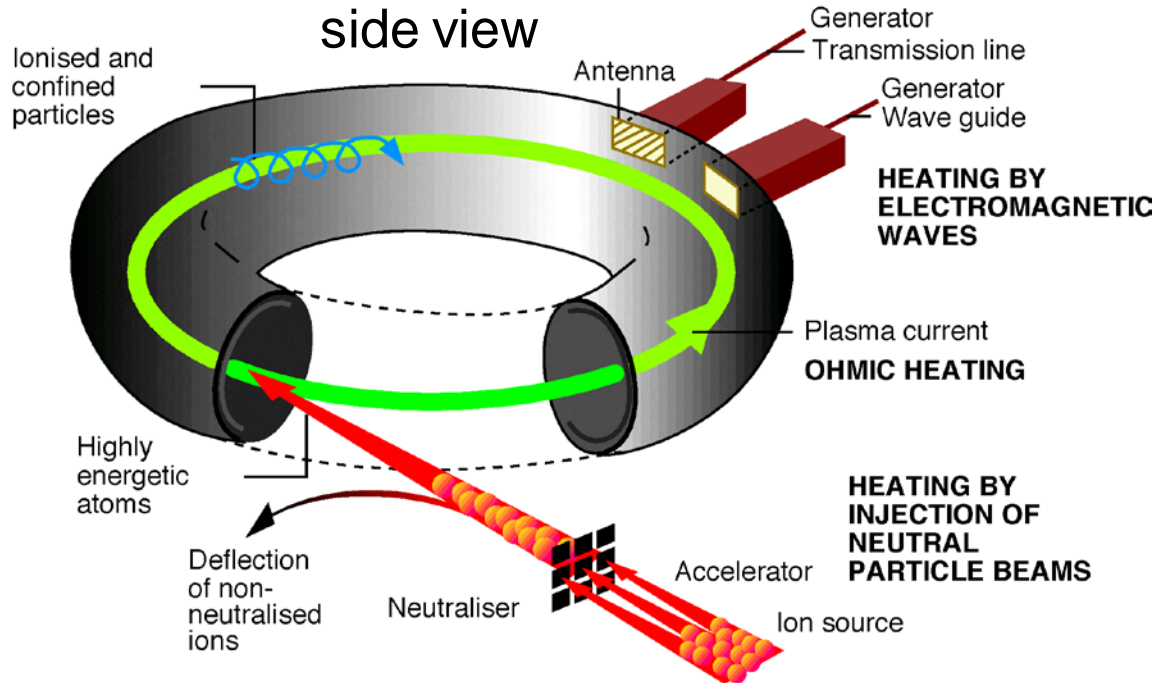
Support Acknowledgement: Luca Guazzotto (University of Rochester), David Pretty (ANU), Rob Akers, Ken McClements, David Muir (CCFE)

Outline

- Anisotropy: equilibrium and stability
 - Expected impact of anisotropy
 - Development of anisotropy into EFIT++ , HELENA
 - Demonstrate impacts of anisotropy on J_ϕ , plasma parameters
 - Development of MHD single adiabatic stability model
 - Compute impact on MAST equilibrium, stability
 - Future directions
- Multiple Relaxed Region MHD model
 - resolves chaotic field regions, islands, flux surfaces in fully 3D plasmas
 - Stepped Pressure Equilibrium Code.
 - Demonstrate two interface model to describe helical plasmas in reverse field pinches
 - Highlight some recent progress
 - Future directions
- Conclusions

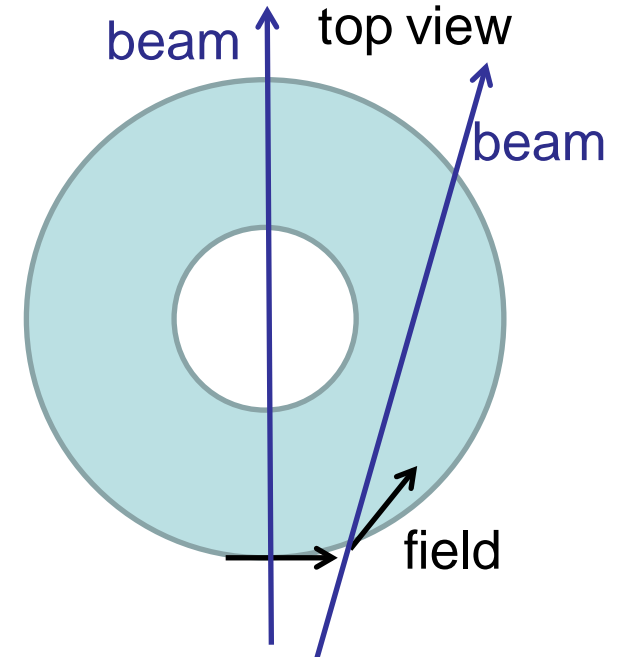
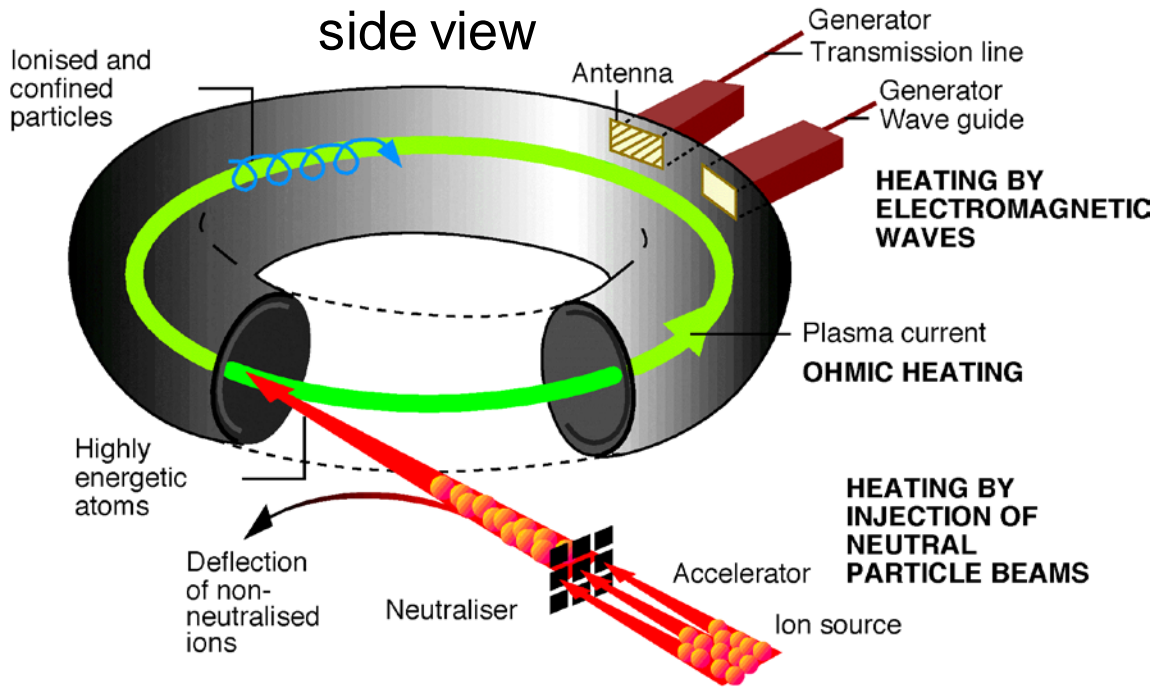
“MHD with anisotropy in velocity, pressure”

- Pressure different parallel and perpendicular to field due mainly to *directed* neutral beam injection



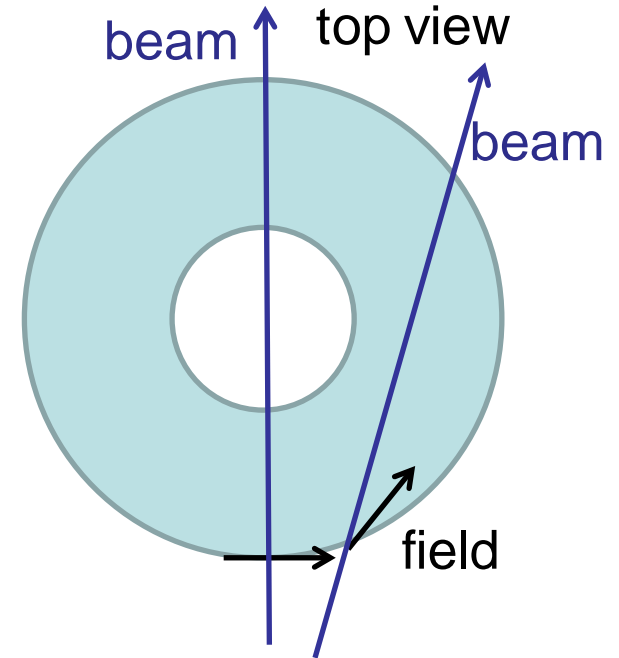
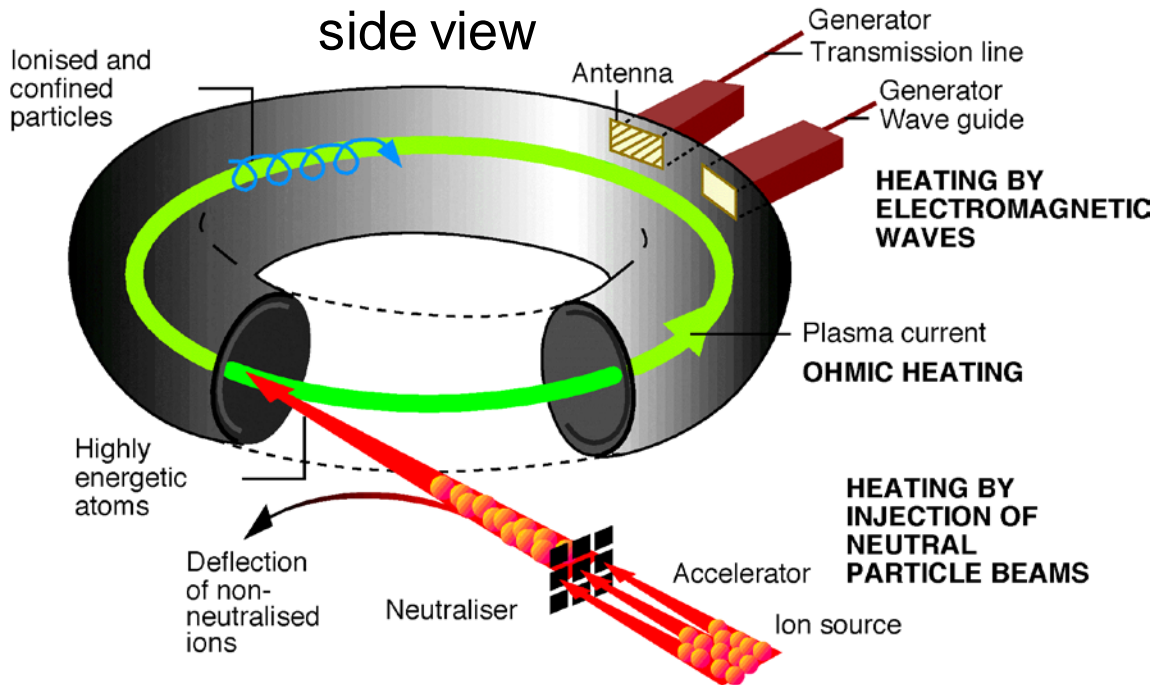
“MHD with anisotropy in velocity, pressure”

- Pressure different parallel and perpendicular to field due mainly to *directed* neutral beam injection



“MHD with anisotropy in velocity, pressure”

- Pressure different parallel and perpendicular to field due mainly to *directed* neutral beam injection



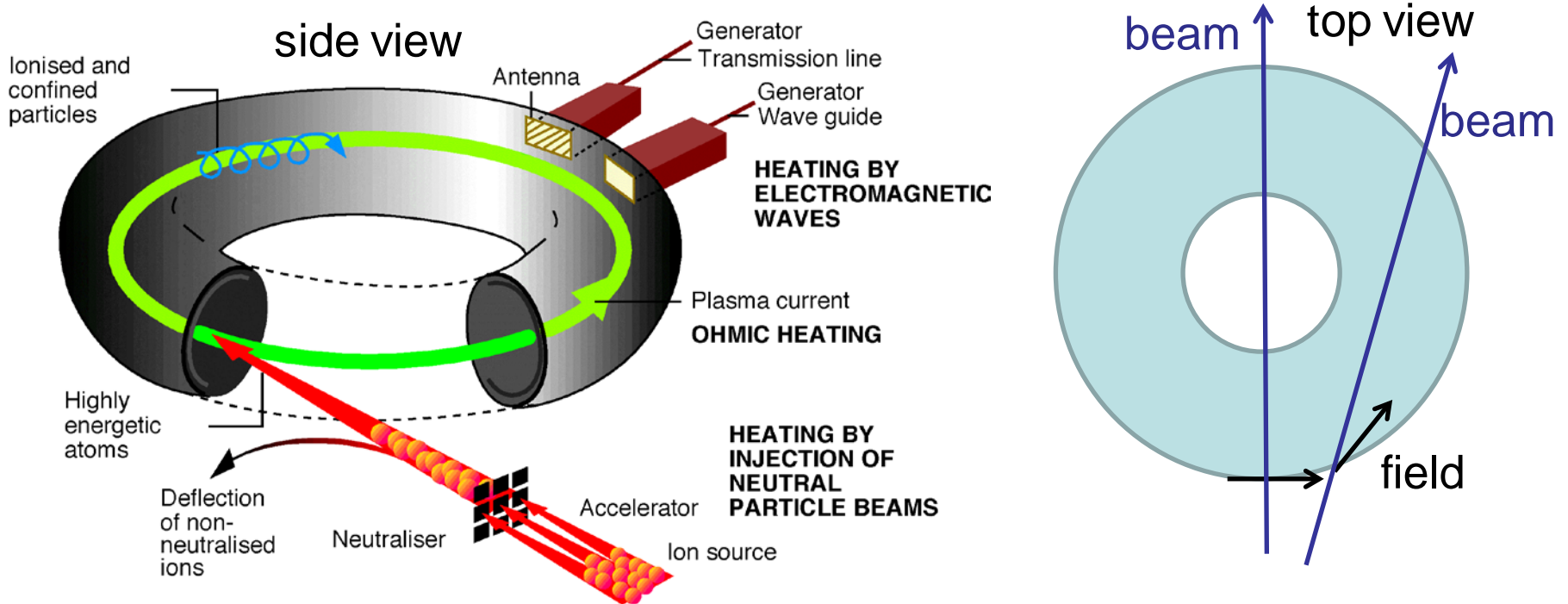
⇒ Pressure is a tensor

$$\bar{\mathbf{P}} = p_{\perp} \bar{\mathbf{I}} + \Delta \mathbf{B}\mathbf{B} / \mu_0,$$

$$\Delta = \frac{\mu_0 (p_{\parallel} - p_{\perp})}{B^2}$$

“MHD with anisotropy in velocity, pressure”

- Pressure different parallel and perpendicular to field due mainly to *directed* neutral beam injection



⇒ Pressure is a tensor $\bar{\mathbf{P}} = p_{\perp} \bar{\mathbf{I}} + \Delta \mathbf{B}\mathbf{B} / \mu_0, \quad \Delta = \frac{\mu_0 (p_{\parallel} - p_{\perp})}{B^2}$

- Momentum

$$\rho \left(\frac{\partial \mathbf{v}}{\partial t} + (\mathbf{v} \cdot \nabla) \cdot \mathbf{v} \right) = -\nabla \cdot \bar{\mathbf{P}} + \mathbf{J} \times \mathbf{B}$$

Expected impact of anisotropy

- Small angle θ_b between beam, field $\Rightarrow p_{||} > p_{\perp}$
- Beam orthogonal to field, $\theta_b = \pi/2 \Rightarrow p_{\perp} > p_{||}$
- If $p_{||}$ sig. enhanced by beam, $p_{||}$ surfaces distorted and displaced inward relative to flux surfaces

[Cooper et al, Nuc. Fus. 20(8), 1980]

- If $p_{\perp} > p_{||}$, an increase will occur in centrifugal shift :

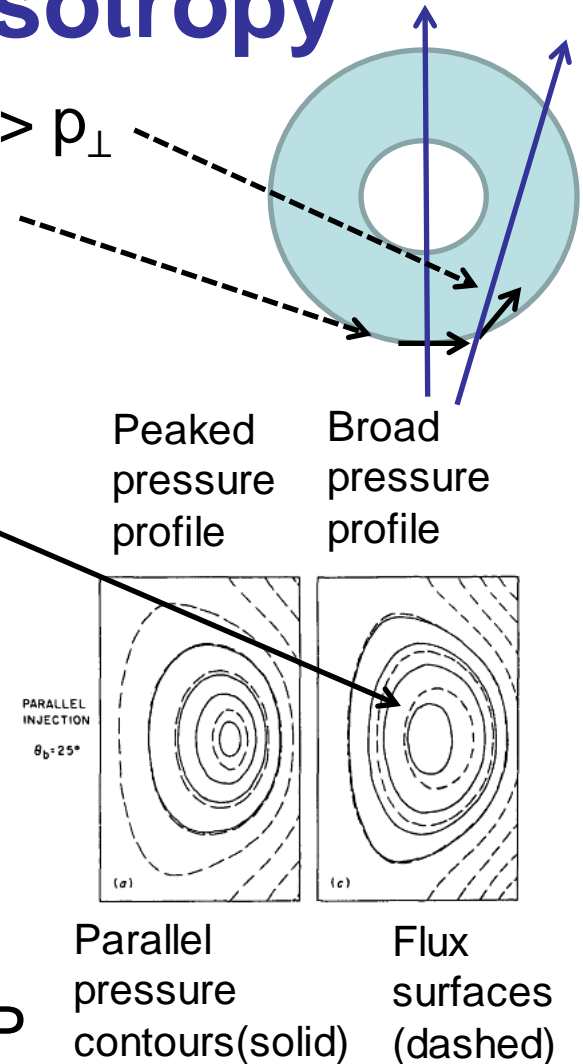
[R. Iacono, A. Bondeson, F. Troyon, and R. Gruber, Phys. Fluids B 2 (8). August 1990]

- Compute p_{\perp} and $p_{||}$ from moments of distribution function, computed by TRANSP

[M J Hole, G von Nessi, M Fitzgerald, K G McClements, J Svensson, PPCF 53 (2011) 074021]

- Infer p_{\perp} from diamagnetic current \mathbf{J}_{\perp}

[see V. Pustovitov, PPCF 52 065001, 2010 and references therein]



MHD with rotation & anisotropy

- Inclusion of anisotropy and flow in equilibrium MHD equations

[R. Iacono, et al Phys. Fluids B 2 (8). 1990]

$$\nabla \cdot (\rho \mathbf{v}) = 0, \quad \rho \mathbf{v} \cdot \nabla \mathbf{v} = \mathbf{J} \times \mathbf{B} - \nabla \cdot \bar{\mathbf{P}}, \quad \nabla \cdot \mathbf{B} = 0$$

$$\mu_0 \mathbf{J} = \nabla \times \mathbf{B}, \quad \nabla \times (\mathbf{v} \times \mathbf{B}) = 0,$$

$$\bar{\mathbf{P}} = p_{\perp} \bar{\mathbf{I}} + \Delta \mathbf{B} \mathbf{B} / \mu_0, \quad \Delta = \frac{\mu_0 (p_{\parallel} - p_{\perp})}{B^2}$$

MHD with rotation & anisotropy

- Inclusion of anisotropy and flow in equilibrium MHD equations

[R. Iacono, et al Phys. Fluids B 2 (8). 1990]

$$\nabla \cdot (\rho \mathbf{v}) = 0, \quad \rho \mathbf{v} \cdot \nabla \mathbf{v} = \mathbf{J} \times \mathbf{B} - \nabla \cdot \bar{\mathbf{P}}, \quad \nabla \cdot \mathbf{B} = 0$$

$$\mu_0 \mathbf{J} = \nabla \times \mathbf{B}, \quad \nabla \times (\mathbf{v} \times \mathbf{B}) = 0,$$

$$\bar{\mathbf{P}} = p_{\perp} \bar{\mathbf{I}} + \Delta \mathbf{B} \mathbf{B} / \mu_0, \quad \Delta = \frac{\mu_0 (p_{\parallel} - p_{\perp})}{B^2}$$

- Frozen flux gives velocity plus axis-symmetry

$$\mathbf{v} = \frac{\psi'_M(\psi)}{\rho} \mathbf{B} - R \phi'_E(\psi) \mathbf{e}_{\phi}.$$

Equilibrium eqn becomes:

$$\nabla \cdot \left[\tau \left(\frac{\nabla \psi}{R^2} \right) \right] = - \frac{\partial p_{\parallel}}{\partial \psi} - \rho H'_M(\psi) + \rho \frac{\partial W}{\partial \psi} - I'_M(\psi) \frac{I}{R^2} - \psi''_M(\psi) \mathbf{v} \cdot \mathbf{B} + R \rho v_{\phi} \phi''_E(\psi)$$

$$I = RB_{\phi}$$

$$I_M(\psi) = \tau I - \mu_0 R^2 \psi'_M(\psi) \phi'_E(\psi)$$

$$H_M(\psi) = W_M(\rho, B, \psi) - \frac{1}{2} [R \phi'_E(\psi)]^2 + \frac{1}{2} \left[\frac{\psi'_M(\psi) B}{\rho} \right]^2,$$

$$\left\{ I_M(\psi), \psi_M(\psi), \phi_E(\psi), H_M(\psi), \frac{\partial p_{\parallel}}{\partial \psi}, \frac{\partial W}{\partial \psi} \right\}$$

Set of 6 profile constraints

$$\tau = 1 - \Delta - \mu_0 (\psi'_M)^2 / \rho,$$

Neglect poloidal flow

- Suppose $\mathbf{v} = -R\phi'_E(\psi)\mathbf{e}_\phi = R\Omega(\psi)\mathbf{e}_\phi \Rightarrow F(\psi) = I_M(\psi)/\tau$

and equilibrium eqn becomes:

$$\nabla \cdot \left[(1-\Delta) \left(\frac{\nabla \psi}{R^2} \right) \right] = -\frac{\partial p_\parallel}{\partial \psi} - \rho H'(\psi) + \rho \frac{\partial W}{\partial \psi} - \frac{F'(\psi)F'(\psi)}{R^2(1-\Delta)} + R^2 \rho \Omega(\psi) \Omega'(\psi)$$

Set of 5 profile constraints

$$\left\{ F(\psi), \Omega(\psi), H(\psi), \frac{\partial p_\parallel}{\partial \psi}, \frac{\partial W}{\partial \psi} \right\}$$

- $\partial W / \partial \psi$: different for MHD/ double-adiabatic/ guiding centre
- If two temperature Bi-Maxwellian model chosen

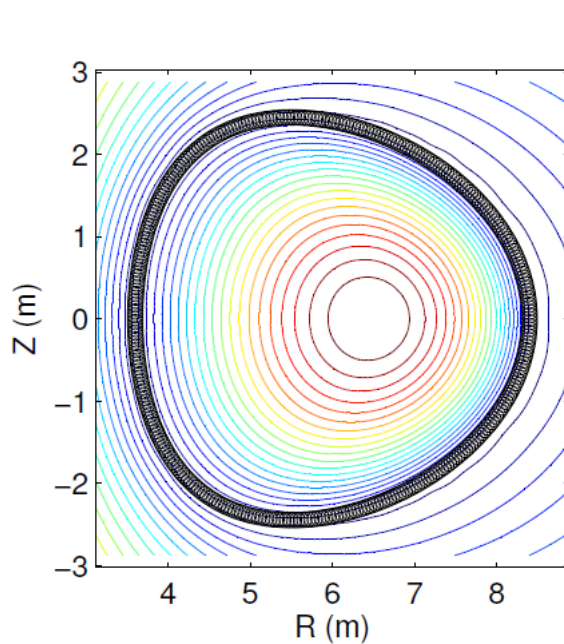
$$p_\parallel(\rho, B\psi) = \frac{k_B}{m} \rho T_\parallel(\psi) \quad p_\perp(\rho, B\psi) = \frac{k_B}{m} \rho T_\perp(\psi) = \frac{k_B}{m} \rho T_\parallel(\psi) \frac{B}{B - \theta(\psi) T_\parallel}$$

$$\left\{ F(\psi), \Omega(\psi), H(\psi), T_\parallel(\psi), \theta(\psi) \right\}$$

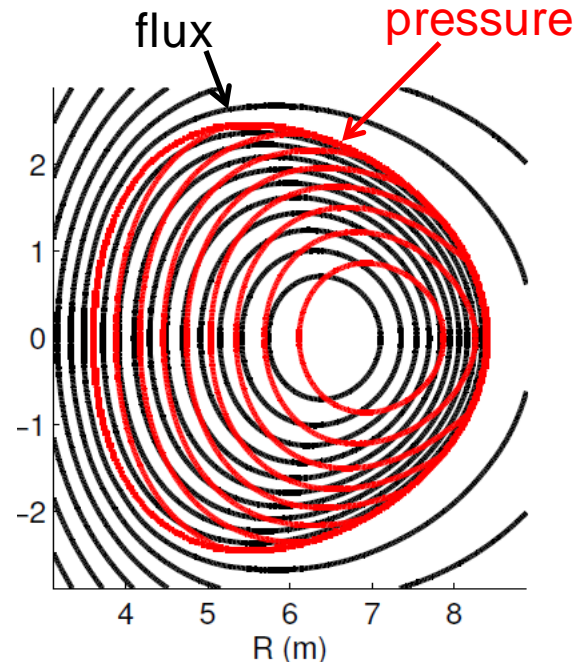
EFIT TENSOR: reconstruction code

- Adds kinetic constraints to magnetic-only constraints of EFIT
- Reveals J_ϕ sensitive to heat transport constraints
- Soloviev benchmarks computed for isotropic, anisotropic and flow cases.
- Used for MAST #13050, #18696
- Installed for both MAST and JET

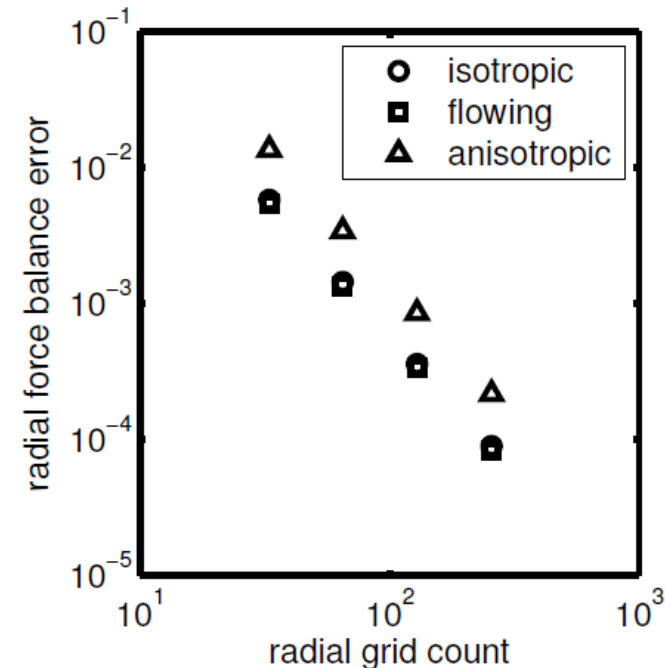
[Fitzgerald, Appel, Hole, Nucl. Fusion **53** (2013) 113040]



Soloviev:
 $\beta_t=0.07$



Extended Soloviev:
 $\beta_t=0.07$, $M_\phi=0.8$, $\Delta=0.004$,



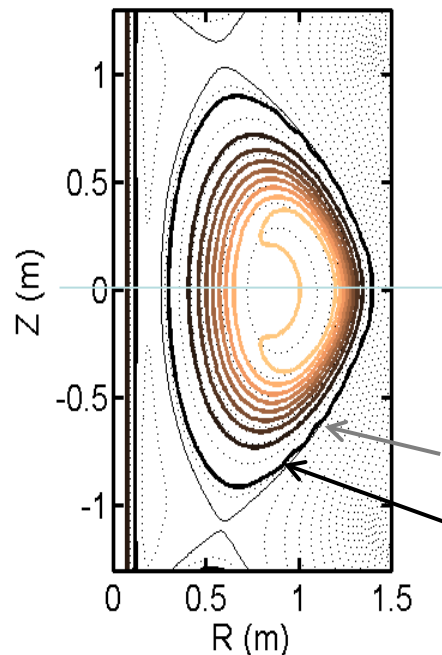
Solution Convergence

HELENA+ATF: parametric scans, stability

- Companion code written to enable stability studies.
- Can be used to study how equilibrium changes with anisotropy

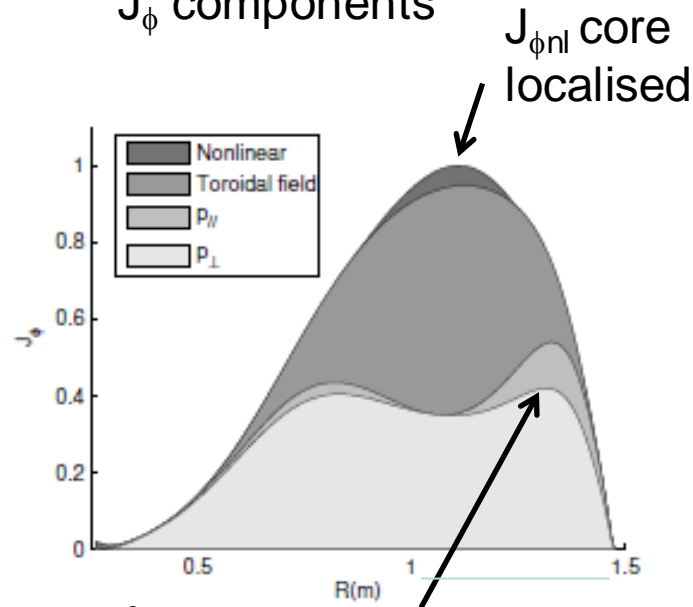
$$J_\phi = \underbrace{R \frac{B_p^2}{B^2} \left(\frac{\partial p_\parallel}{\partial \Psi} \right)_B}_{p_\parallel} + \underbrace{R \frac{B^2 - B_p^2}{B^2} \left(\frac{\partial p_\perp}{\partial \Psi} \right)_B}_{p_\perp} + \underbrace{\frac{1 - \Delta}{2R} \left(\frac{\partial (RB_\phi)^2}{\partial \Psi} \right)_B}_{\text{toroidal field}} - \underbrace{R \nabla \cdot \frac{\Delta \nabla \Psi}{R^2}}_{\text{nonlinear}}$$

MAST-like equilibrium



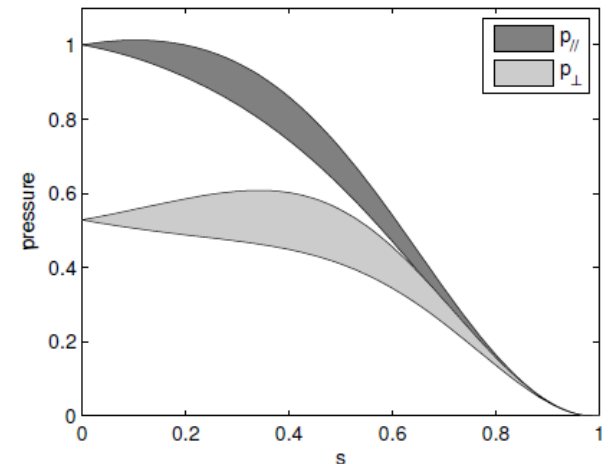
flux
surfaces of constant p_\parallel .

J_ϕ components



$J_{\phi\parallel}$ dominant outboard

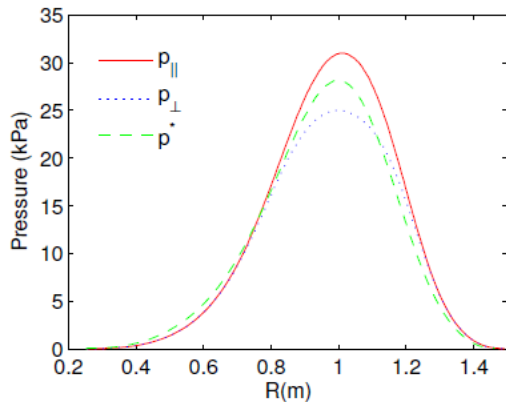
$J_{\phi nl}$ core localised



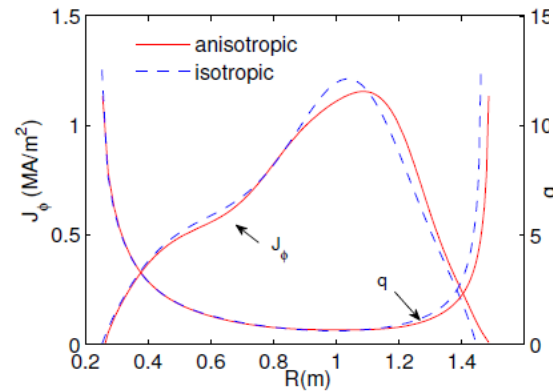
$s \propto \sqrt{r}$

HELENA+ATF: parametric scans, stability

$$J_\varphi = \underbrace{R \frac{B_p^2}{B^2} \left(\frac{\partial p_{\parallel}}{\partial \Psi} \right)_B}_{p_{\parallel}} + \underbrace{R \frac{B^2 - B_p^2}{B^2} \left(\frac{\partial p_{\perp}}{\partial \Psi} \right)_B}_{p_{\perp}} + \underbrace{\frac{1 - \Delta}{2R} \left(\frac{\partial (RB_\varphi)^2}{\partial \Psi} \right)_B}_{\text{toroidal field}} - \underbrace{R \nabla \cdot \frac{\Delta \nabla \Psi}{R^2}}_{\text{nonlinear}}$$



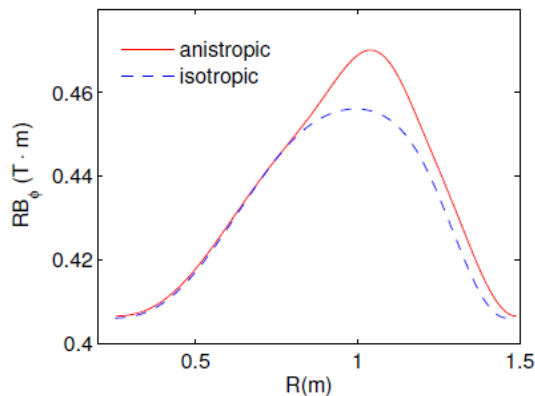
(a)



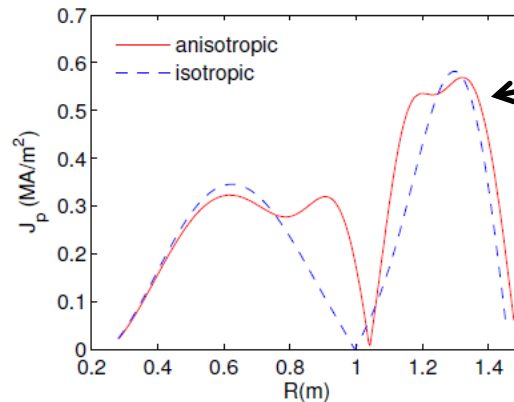
(b)

$$\mu_0 \mathbf{J}_p = \nabla (RB_\varphi) \times \nabla \varphi$$

$$p_{\parallel}/p_{\perp} \approx 1.25$$



(c)

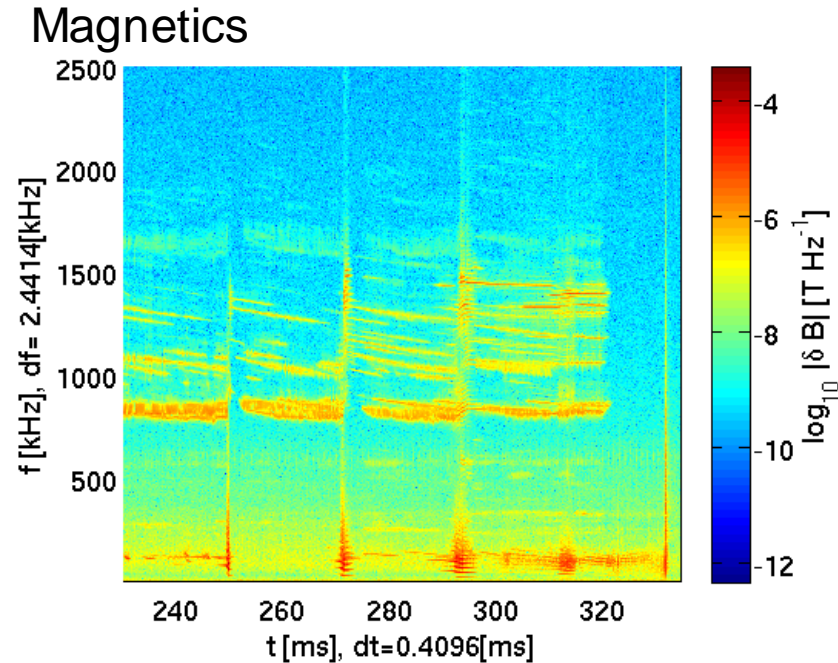
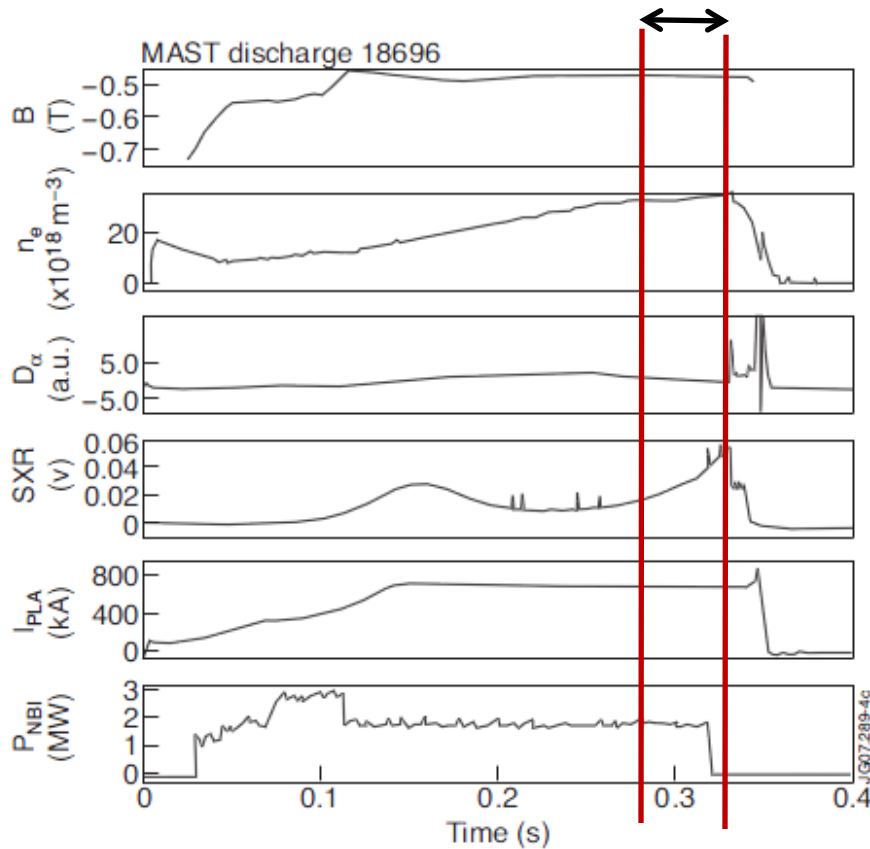


(d)

Most significant difference in \mathbf{J}_p which can effect change in stability

Anisotropy on MAST: #18696

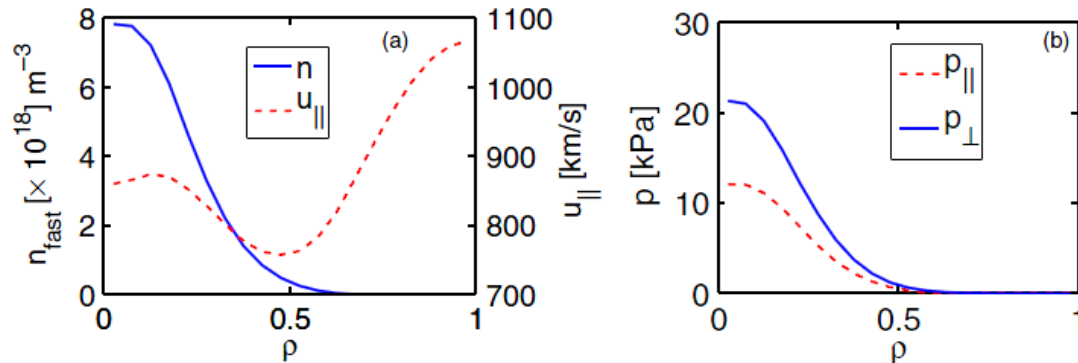
- MAST #18696
- 1.9MW NB heating
- $I_p = 0.7\text{MA}$, $\beta_n=2.5$
- TRANSP simulation available
- Magnetics shows CAEs



[M.P. Gryaznevich et al, Nuc. Fus. 48, 084003, 2008.; Lilley *et al* 35th EPS Conf. Plas.Phys. 9 - 13 June 2008 ECA Vol.32D, P-1.057]

- What is the impact on q profile due to presence of anisotropy and flow?

Beam population $p_{\perp}/p_{\parallel} \approx 1.7$



$$p_{\perp}/p_{\parallel} \approx 1.7$$

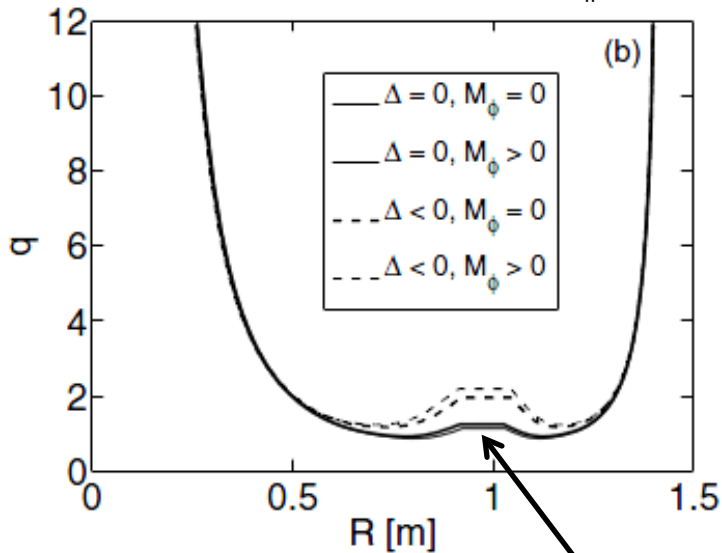
$$\rho = \sqrt{\Phi / \Phi_0}$$

$\Phi =$ toroidal flux

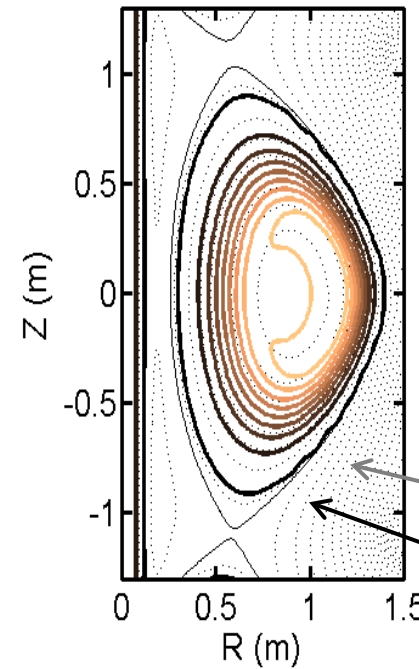
Impact on plasma computed using FLOW, EFIT TENSOR

FLOW scans $\Delta < 0$: $p_{\perp}/p_{\parallel} \approx 1.7$
 $\Delta = 0$: $p_{\perp}/p_{\parallel} = 1$

EFIT++ (TENSOR)



Low grid resolution of FLOW at core



Calculation of MAST #18696 at 290ms.

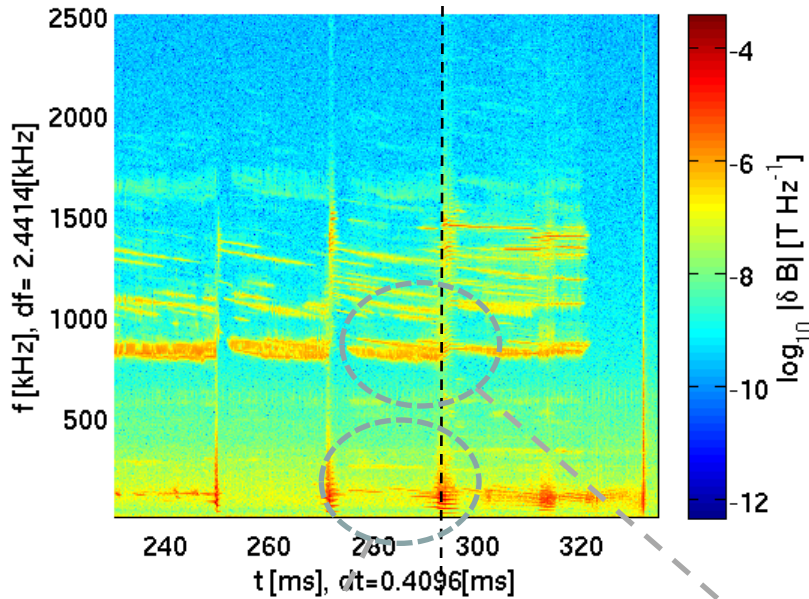
$$p_{\perp} / p_{\parallel} \sim 1.7$$

(slowing down beam particles)

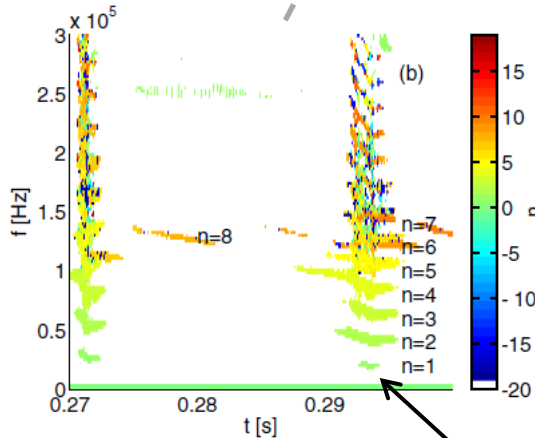
poloidal flux

surfaces of constant p_{\parallel} .

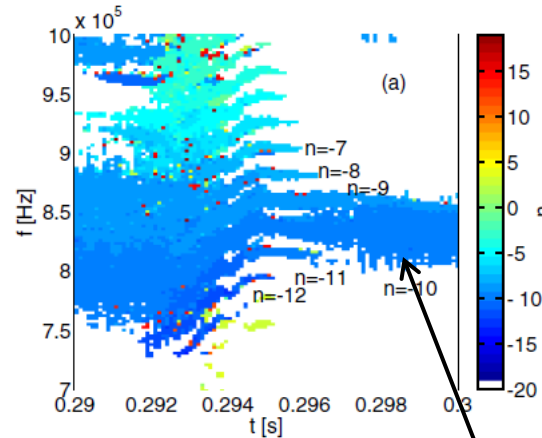
Anisotropy on MAST



- How do predicted mode frequencies change due to changes in q produced by anisotropy and flow?



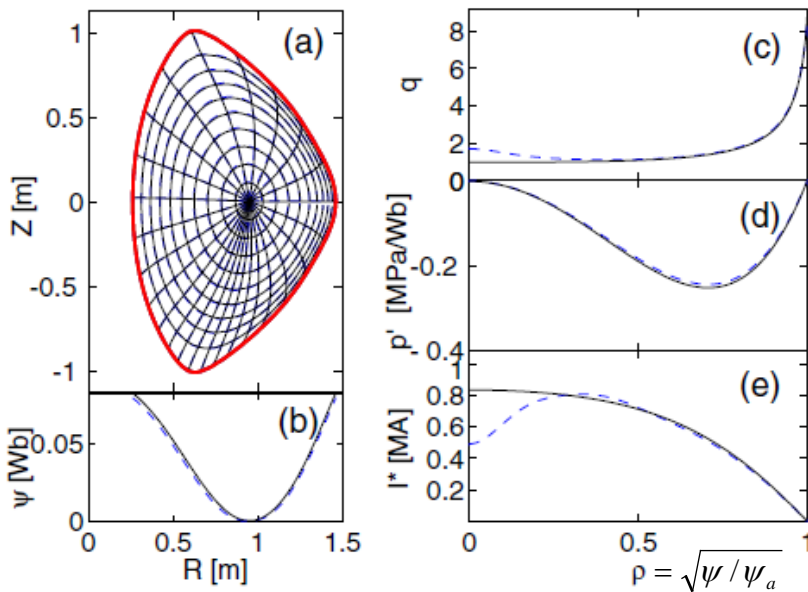
n=1 mode



n=-10 mode

- Appetiser: What is the change in ideal MHD stability of n=1 TAE?

Increased shear gives multiple TAEs: *changes radial structure*

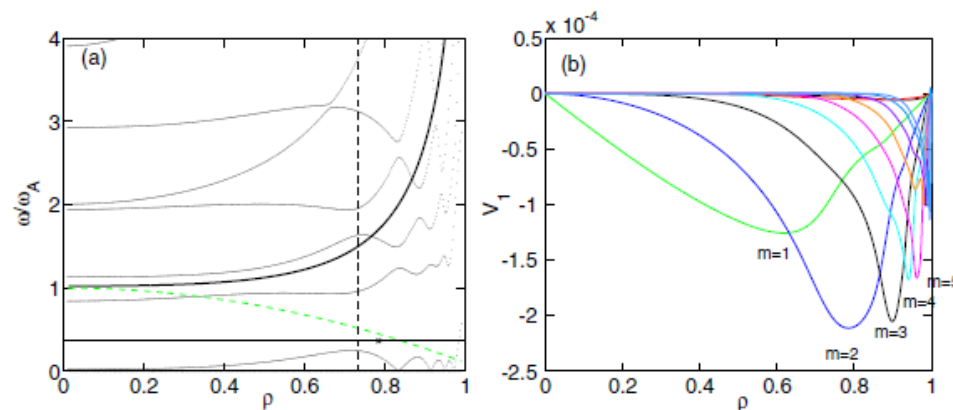


- Reshape plasma to have larger reverse shear

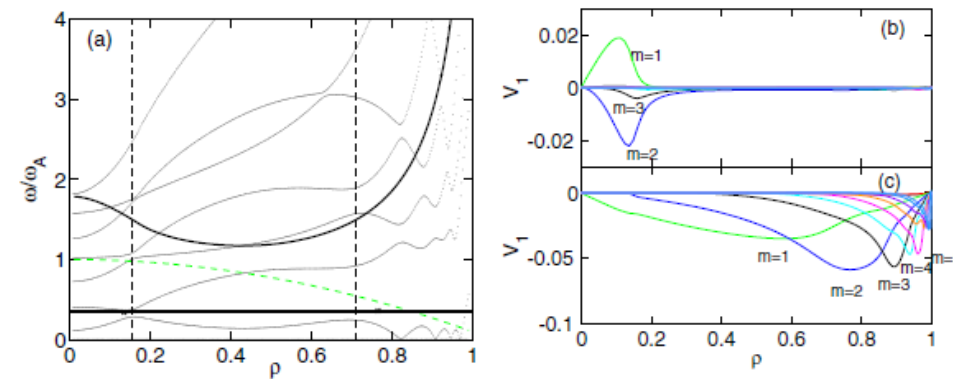
$$I^*(s) \rightarrow I^*(s) + \underbrace{I_0 \exp\left[-\frac{(s-s_0)^2}{2\sigma_0^2}\right]}_{\text{core}} + \underbrace{I_1 \exp\left[-\frac{(s-s_1)^2}{2\sigma_1^2}\right]}_{\text{reverse shear}}$$

I_0, I_1 varied to match $q_0=1.7, q_{\min}=1.24$

[M J Hole, G von Nessi, M Fitzgerald and the MAST team, PPCF, 55 014007, 2013]



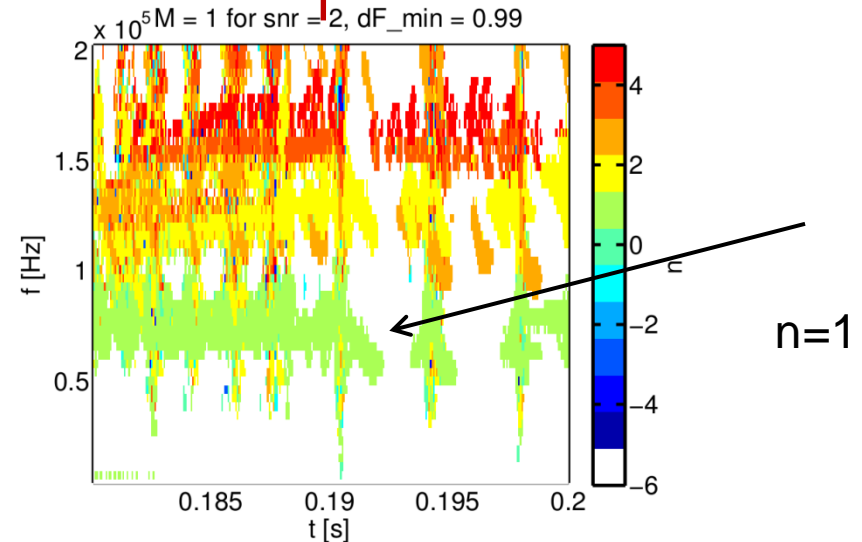
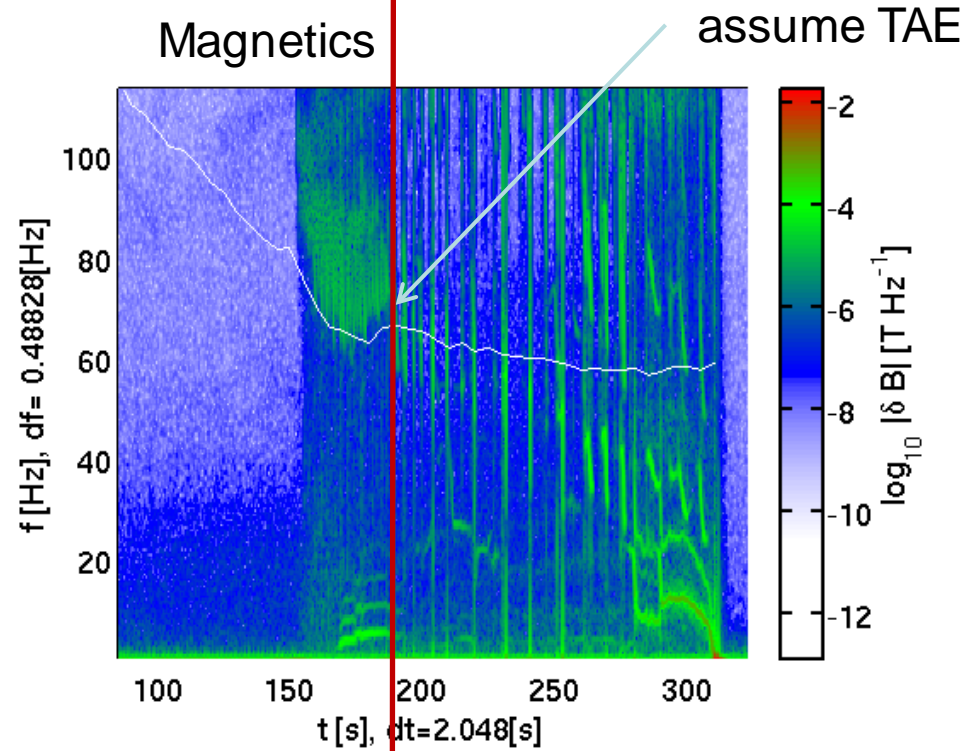
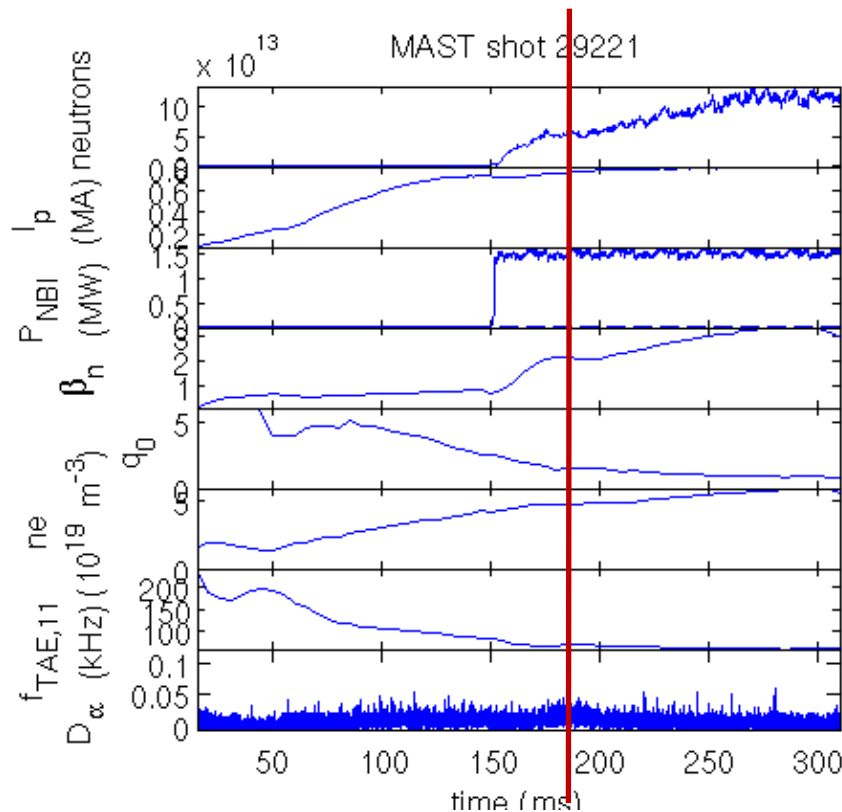
Single global TAE at $(m,n) = (1,1)$



Reverse shear produces second $(m,n) = (1,1)$ odd TAE resonance in the core

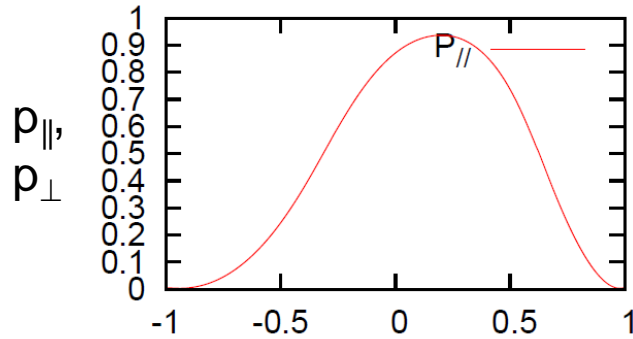
Anisotropy on MAST: #29221

- MAST #29221
- 1.6MW NB heating
- $I_p = 0.9\text{MA}$, $\beta_n \sim 3$
- Magnetics shows TAEs, tearing modes fishbones, long-lived modes

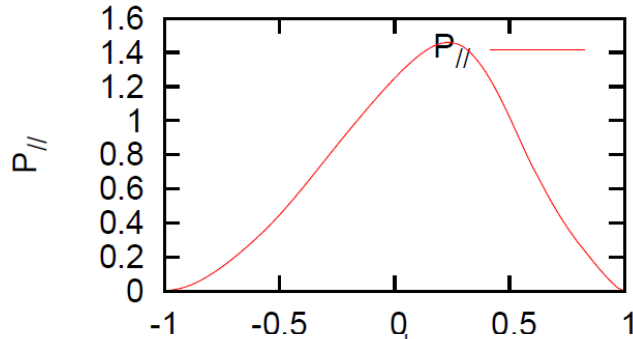


Beam + thermal population: $p_{\parallel} / p_{\perp} \approx 1.4$

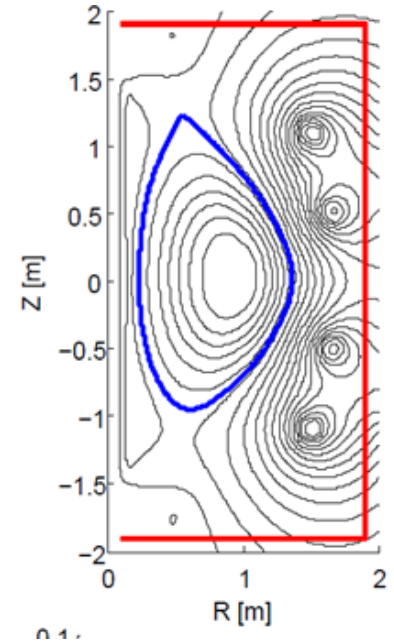
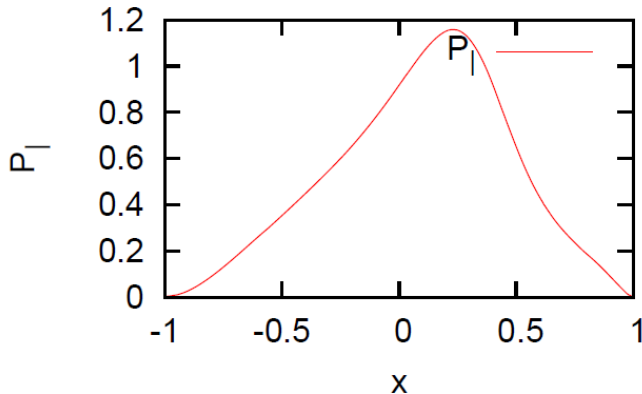
HELENA+ATF / EFIT TENSOR: no flow + p^*



HELENA+ATF / EFIT TENSOR: no flow, anisotropy

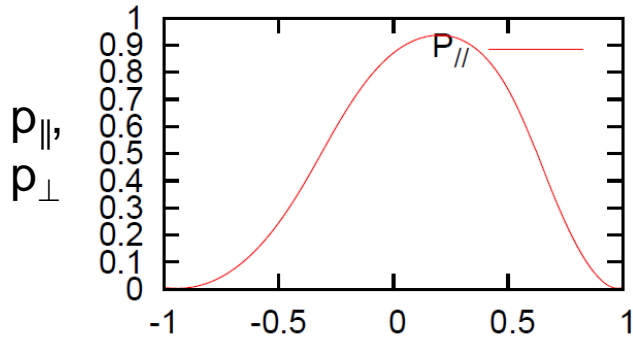


$$p_{\parallel} / p_{\perp} = 1.4 \text{ at } r/R=0.5$$

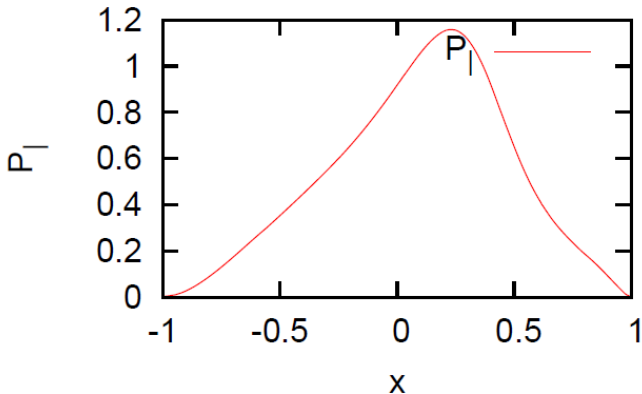
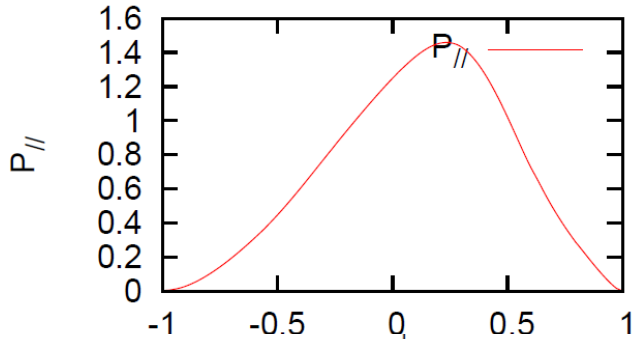


Beam + thermal population: $p_{\parallel} / p_{\perp} \approx 1.4$

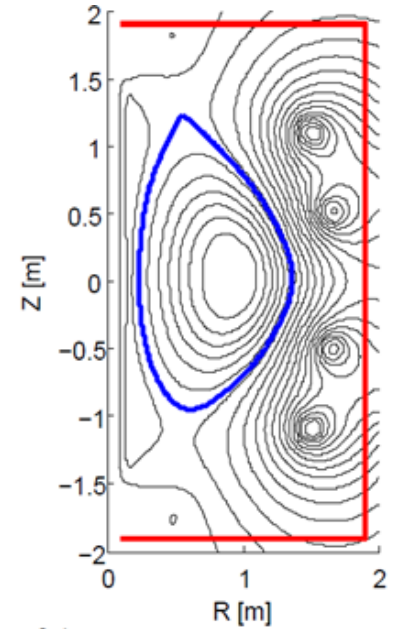
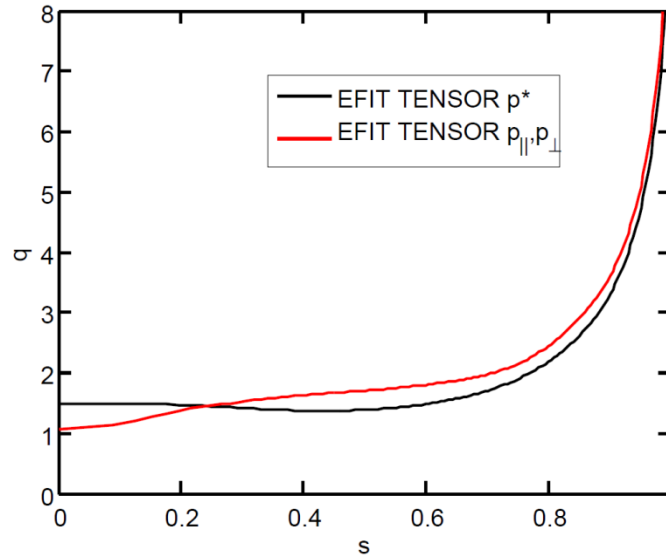
HELENA+ATF / EFIT TENSOR: no flow + p^*



HELENA+ATF / EFIT TENSOR: no flow, anisotropy



$p_{\parallel} / p_{\perp} = 1.4$ at $r/R=0.5$



- What is the impact on stability due to this q profile?

Stability: incompressional

- Normal mode treatment: Linearise around time dependent oscillations of form $\exp[i(\omega t - m\theta - n\phi)]$
- Without compressibility, Mikhailovski (*) show perturbed Lagrangian distribution function is zero, meaning that the Euler perturbed distribution function is

$$\tilde{f} = -\xi_{\perp} \cdot \nabla F$$

The fluid closure equations are*

$$p_{\parallel 1} = -\xi_n \left[\frac{\partial p_{\parallel}}{\partial n} - (p_{\parallel} - p_{\perp}) \frac{\partial \ln B}{\partial n} \right]$$

$$p_{\perp 1} = -\xi_n \left[\frac{\partial p_{\perp}}{\partial n} - (2p_{\perp} + \hat{c}) \frac{\partial \ln B}{\partial n} \right]$$

$$\hat{c} \equiv \sum_s M_s \int \frac{B}{v_{\parallel}} (\mu B)^2 \frac{\partial F_s}{\partial \varepsilon} d\mu d\varepsilon.$$

*A B Mikhailovskii, Instabilities in a confined plasma, IOP publishing (1998)

Stability: compressional

- Using existing model
 - *Double-adiabatic (CGL)*
 - Collisionless, p_{\parallel} and p_{\perp} do **independent** work
 - No streaming particle heat flow
 - Does not reduce to MHD in the isotropic limit

$$\frac{d}{dt} \left(\frac{p_{\perp}}{\rho B} \right) = 0,$$

$$\frac{d}{dt} \left(\frac{p_{\parallel} B^2}{\rho^3} \right) = 0.$$

Stability: compressional

- Using existing model
 - *Double-adiabatic (CGL)*
 - Collisionless, p_{\parallel} and p_{\perp} do **independent** work
 - No streaming particle heat flow
 - Does not reduce to MHD in the isotropic limit
 - *Double-polytropic law*
 - Generalisation of CGL but unclear rationale for choices of adiabatic index γ_{\perp} , γ_{\parallel}

$$\frac{d}{dt} \left(\frac{p_{\perp}}{\rho B} \right) = 0,$$

$$\frac{d}{dt} \left(\frac{p_{\parallel} B^2}{\rho^3} \right) = 0.$$

$$\frac{d}{dt} \left(\frac{p_{\perp}}{\rho B^{\gamma_{\perp}-1}} \right) = 0$$

$$\frac{d}{dt} \left(\frac{p_{\parallel} B^{\gamma_{\parallel}-1}}{\rho^{\gamma_{\parallel}}} \right) = 0$$

Stability: compressional

- Using existing model
 - *Double-adiabatic (CGL)*
 - Collisionless, p_{\parallel} and p_{\perp} do **independent** work
 - No streaming particle heat flow
 - Does not reduce to MHD in the isotropic limit

$$\frac{d}{dt} \left(\frac{p_{\perp}}{\rho B} \right) = 0,$$

$$\frac{d}{dt} \left(\frac{p_{\parallel} B^2}{\rho^3} \right) = 0.$$

- *Double-polytropic law*
 - Generalisation of CGL but unclear rationale for choices of adiabatic index $\gamma_{\perp}, \gamma_{\parallel}$

$$\frac{d}{dt} \left(\frac{p_{\perp}}{\rho B^{\gamma_{\perp}-1}} \right) = 0$$
$$\frac{d}{dt} \left(\frac{p_{\parallel} B^{\gamma_{\parallel}-1}}{\rho^{\gamma_{\parallel}}} \right) = 0$$

- New extension to MHD

- *Single adiabatic (SA) model*
 - p_{\parallel} and p_{\perp} doing **joint** work
 - Accounting for the isotropic part of the perturbation
 - Can reduce to MHD in isotropic limit

$$\tilde{\mathbf{P}} \rightarrow \tilde{p}\mathbf{I}$$

[Fitzgerald, Hole, Qu, submitted PPCF 08/09/2014]

Stability: compressional

- Using existing model
 - *Double-adiabatic (CGL)*
 - Collisionless, p_{\parallel} and p_{\perp} do **independent** work
 - No streaming particle heat flow
 - Does not reduce to MHD in the isotropic limit

$$\frac{d}{dt} \left(\frac{p_{\perp}}{\rho B} \right) = 0,$$

$$\frac{d}{dt} \left(\frac{p_{\parallel} B^2}{\rho^3} \right) = 0.$$

- *Double-polytropic law*
 - Generalisation of CGL but unclear rationale for choices of adiabatic index $\gamma_{\perp}, \gamma_{\parallel}$

$$\frac{d}{dt} \left(\frac{p_{\perp}}{\rho B^{\gamma_{\perp}-1}} \right) = 0$$
$$\frac{d}{dt} \left(\frac{p_{\parallel} B^{\gamma_{\parallel}-1}}{\rho^{\gamma_{\parallel}}} \right) = 0$$

- New extension to MHD

- *Single adiabatic (SA) model*
 - p_{\parallel} and p_{\perp} doing **joint** work
 - Accounting for the isotropic part of the perturbation
 - Can reduce to MHD in isotropic limit

$$\tilde{\mathbf{P}} \rightarrow \tilde{p}\mathbf{I}$$

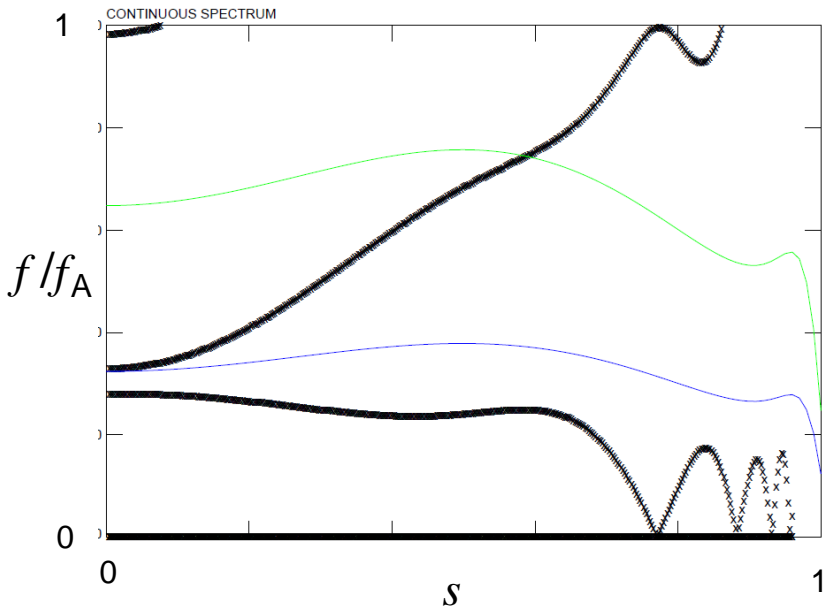
[Fitzgerald, Hole, Qu, submitted PPCF 08/09/2014]

- Implemented both SA and CGL in CSCAS (CSMIS-A) and MISHKA (MISHKA-A)

Incompressible continuum for MAST

isotropic

$n=1, \gamma=0$

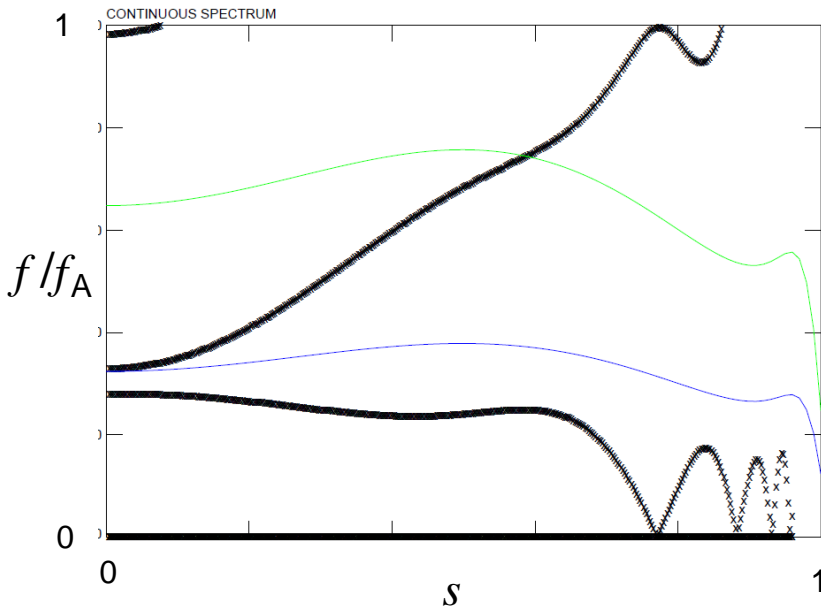


$$R_{mag} = f_A \text{ at magnetic axis} = 280\text{kHz}$$

Incompressible continuum for MAST

isotropic

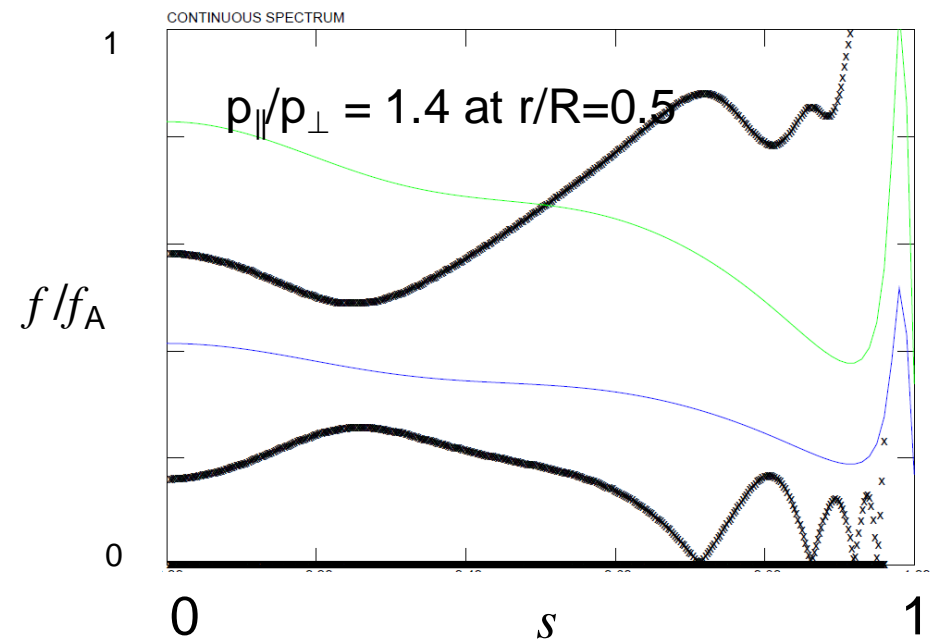
$n=1, \gamma=0$



$R_{mag} =$
 f_A at magnetic axis = 280kHz

anisotropic

$n=1, \gamma=0$



$R_{mag} =$
 f_A at magnetic axis = 260kHz

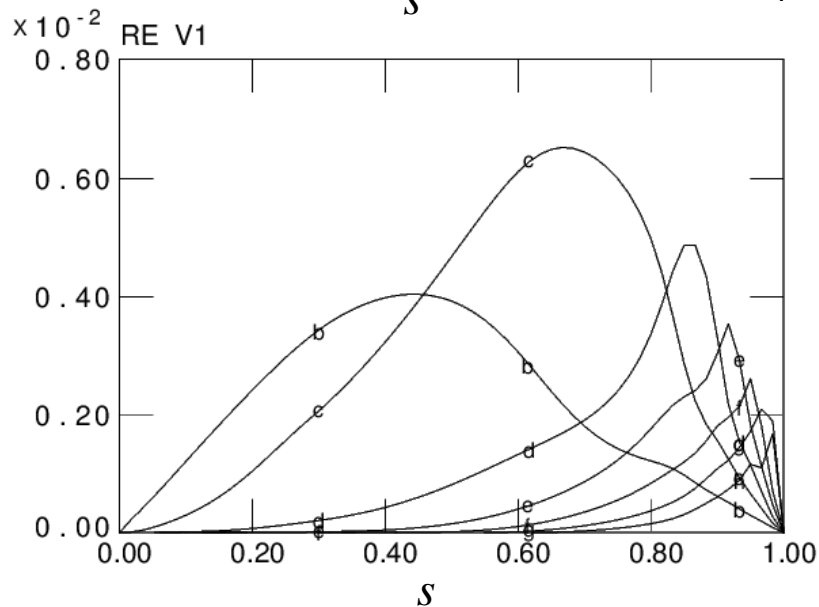
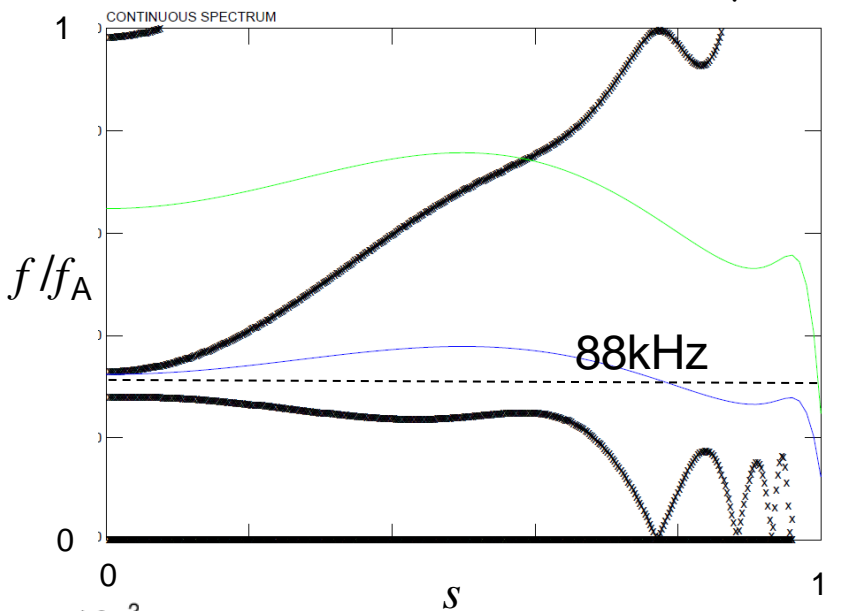
isotropic $\Delta f_{TAE} <$ anisotropic Δf_{TAE}

\Rightarrow anisotropic modes likely to have less continuum damping

Anisotropic mode profile broader

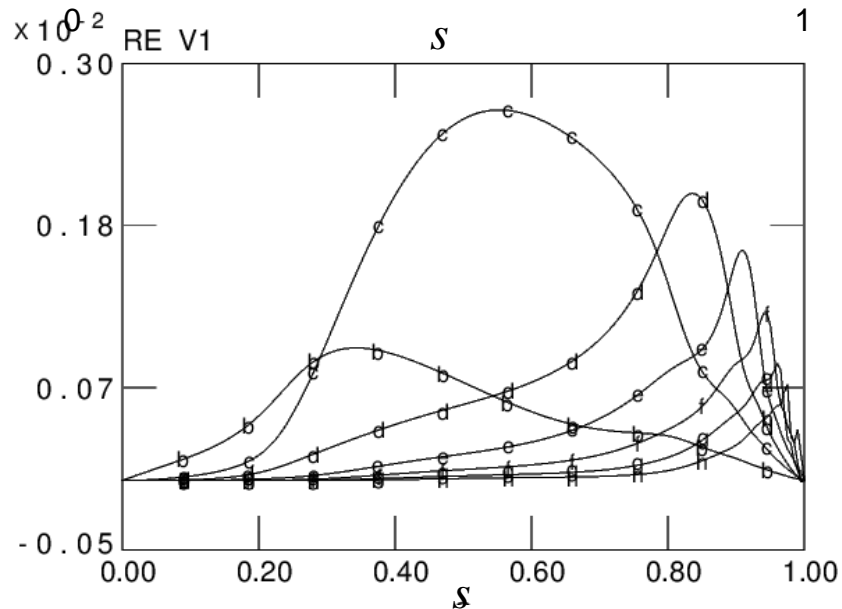
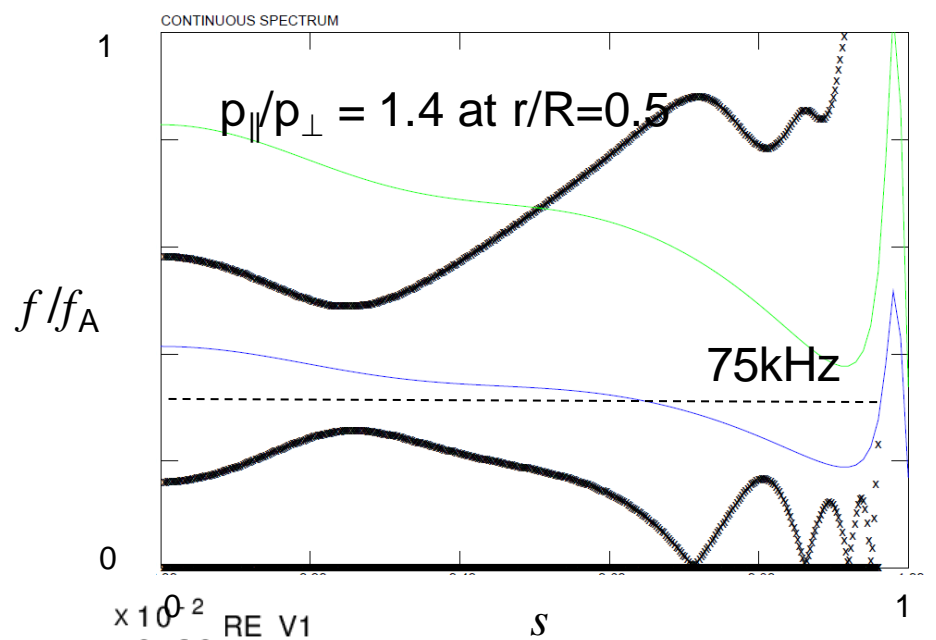
isotropic

$n=1, \gamma=0$



anisotropic

$n=1, \gamma=0$



Ongoing work in Anisotropy and Flow

- Demonstrated significant anisotropy in MAST, $0.6 < p_{\parallel} / p_{\perp} < 1.4$
 - Can produce significant change in equilibrium
 - change central safety factor (helicity) by up to 15%
[M J Hole *et al* PPCF **53**, 074021, 2011]
 - Can produce significant poloidal current.
[Qu, Fitzgerald, Hole, Plasma Phys. Control. Fusion **56** (2014) 075007]
 - Can change stability:
 - Through change in q in ideal MHD – introduce multiple gap modes
[M J Hole *et al*, PPCF, **55** 014007, 2013]
 - In incompressible plasmas, lead to: wider gaps, reduced continuum damping, broader radial structure.
 - Developed new Single Adiabatic model. Implemented in MISHKA, CSCAS. [Fitzgerald, Hole, Qu, submitted PPCF 08/09/2014]

To do...

- Couple EFIT TENSOR, MISHKA to wave-particle interaction code HAGIS for self-consistent evolution
- Explore wave-particle interaction new physics

Outline

- Anisotropy: equilibrium and stability
 - Expected impact of anisotropy
 - Development of anisotropy into EFIT++ , HELENA
 - Demonstrate impacts of anisotropy on J_ϕ , plasma parameters
 - Development of MHD single adiabatic stability model
 - Compute impact on MAST equilibrium, stability
 - Future directions
- Multiple Relaxed Region MHD model
 - resolves chaotic field regions, islands, flux surfaces in fully 3D plasmas
 - Stepped Pressure Equilibrium Code.
 - Demonstrate two interface model to describe helical plasmas in reverse field pinches
 - Highlight some recent progress
 - Future directions
- Conclusions

3D equilibria in toroidal plasmas

- Simplest model to approximate global, macroscopic force-balance is magnetohydrodynamics (MHD).

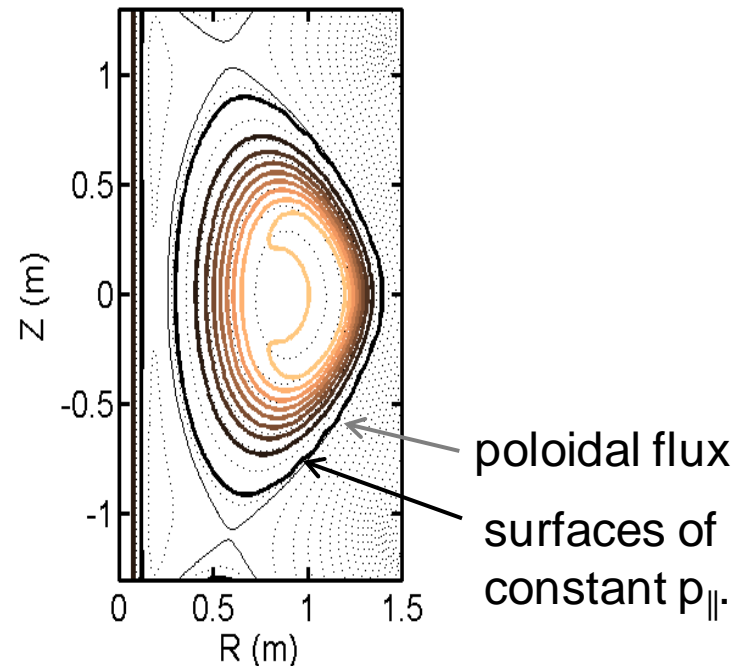
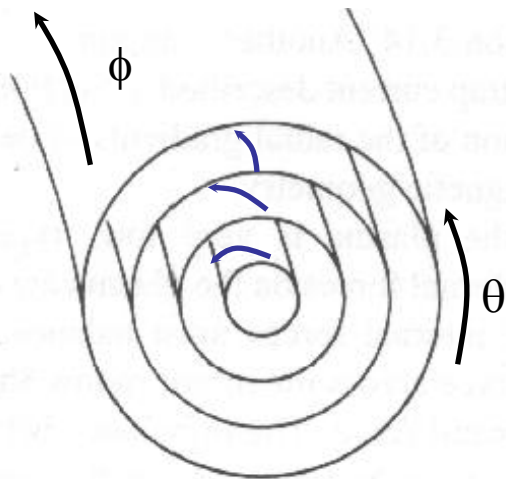
$$\nabla p = \mathbf{J} \times \mathbf{B}, \quad \nabla \times \mathbf{B} = \mathbf{J}, \quad \nabla \cdot \mathbf{B} = 0$$

3D equilibria in toroidal plasmas

- Simplest model to approximate global, macroscopic force-balance is magnetohydrodynamics (MHD).

$$\nabla p = \mathbf{J} \times \mathbf{B}, \quad \nabla \times \mathbf{B} = \mathbf{J}, \quad \nabla \cdot \mathbf{B} = 0$$

- Toroidal symmetry \Rightarrow field lies in nested flux surfaces

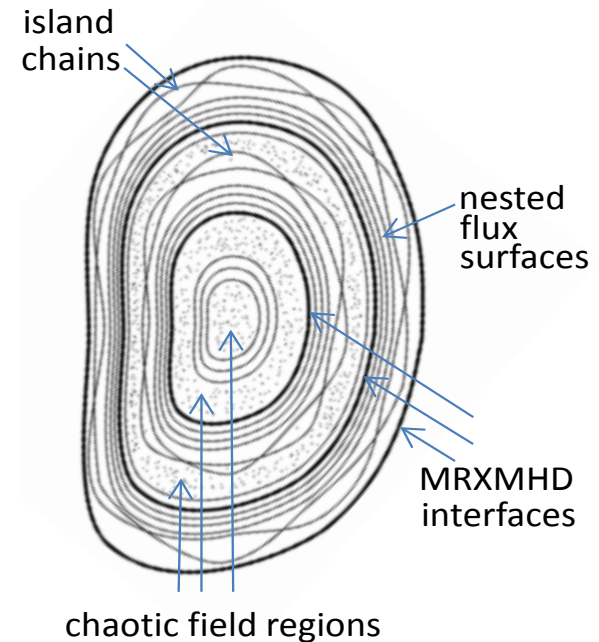


3D equilibria in toroidal plasmas

- Simplest model to approximate global, macroscopic force-balance is magnetohydrodynamics (MHD).

$$\nabla p = \mathbf{J} \times \mathbf{B}, \quad \nabla \times \mathbf{B} = \mathbf{J}, \quad \nabla \cdot \mathbf{B} = 0$$

- Non-axisymmetric \Rightarrow field does **not** lie in nested flux surfaces **unless** surface currents allowed.

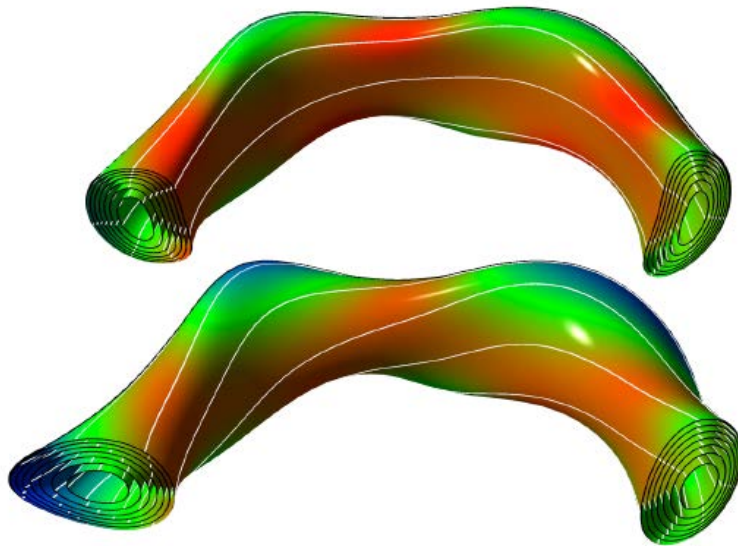


3D equilibria in toroidal plasmas

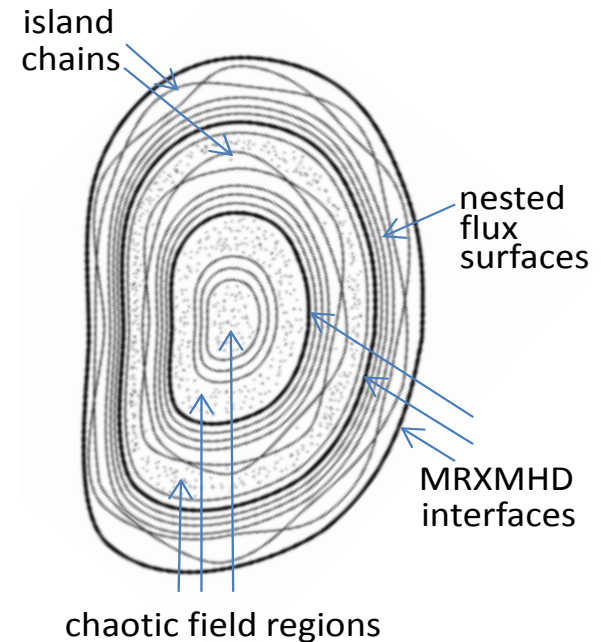
- Simplest model to approximate global, macroscopic force-balance is magnetohydrodynamics (MHD).

$$\nabla p = \mathbf{J} \times \mathbf{B}, \quad \nabla \times \mathbf{B} = \mathbf{J}, \quad \nabla \cdot \mathbf{B} = 0$$

- Non-axisymmetric \Rightarrow field does **not** lie in nested flux surfaces **unless** surface currents allowed.
- Existing 3D solvers (e.g. VMEC) assume nested flux surfaces.



[CTH stellarator, Hanson et al, IAEA 2012]



3D equilibria in toroidal plasmas

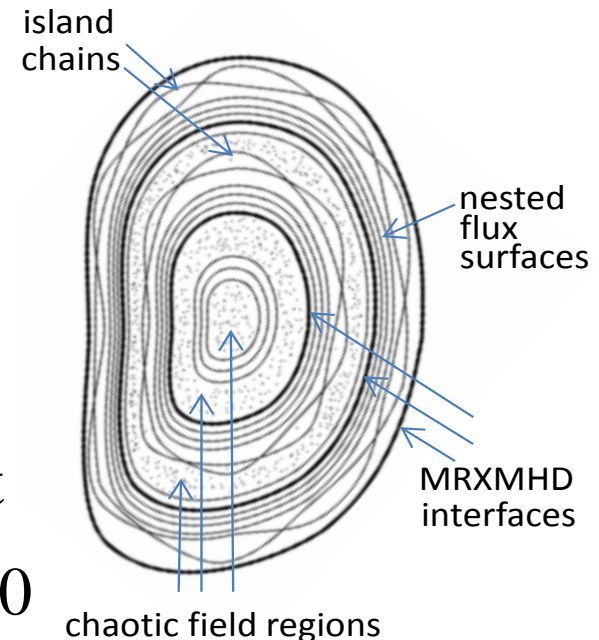
- Simplest model to approximate global, macroscopic force-balance is magnetohydrodynamics (MHD).

$$\nabla p = \mathbf{J} \times \mathbf{B}, \quad \nabla \times \mathbf{B} = \mathbf{J}, \quad \nabla \cdot \mathbf{B} = 0$$

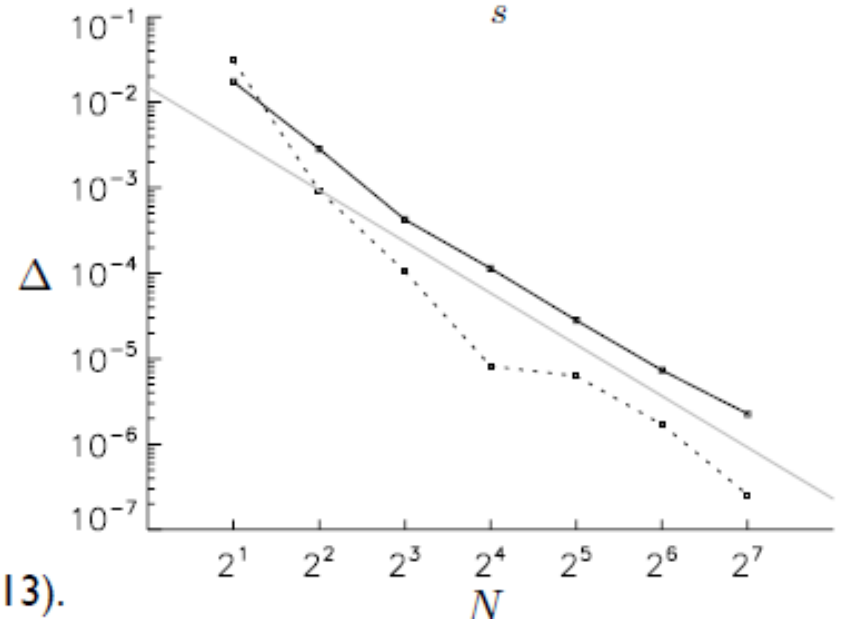
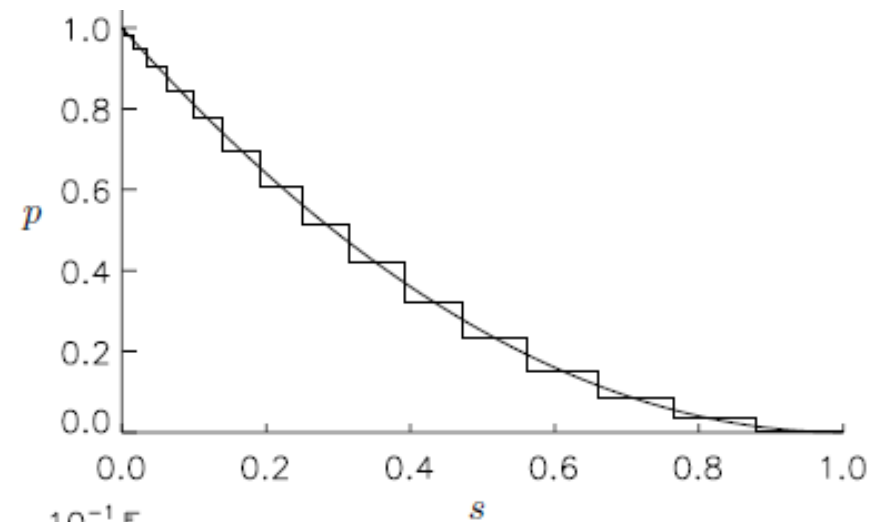
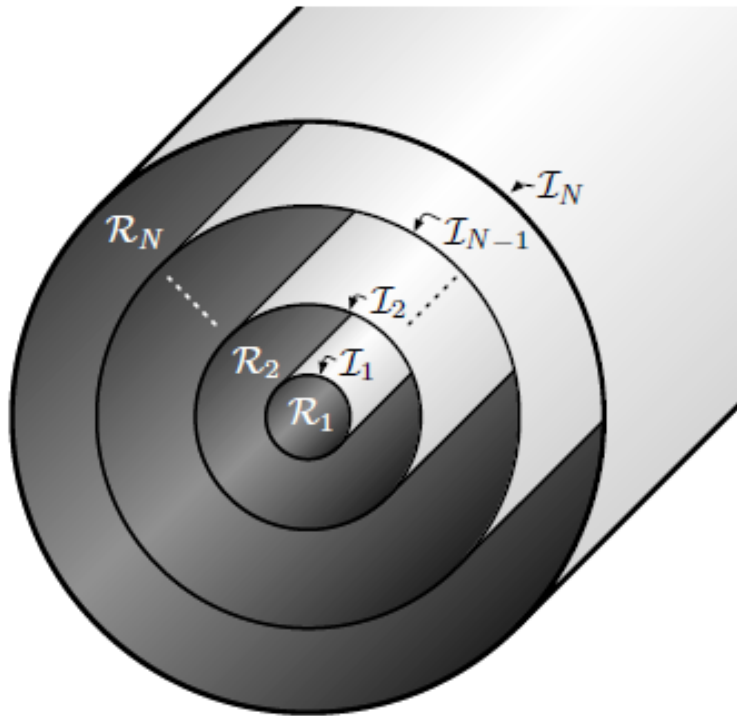
- Non-axisymmetric \Rightarrow field does **not** lie in nested flux surfaces **unless** surface currents allowed.
- Existing 3D solvers (e.g. VMEC) assume nested flux surfaces.
- Generalised Taylor relaxation model: Multiple Relaxed Region MHD (MRXMHD) supports full complexity of field: nested flux surfaces, magnetic islands, chaotic regions.

Volume: $\nabla \times \mathbf{B} = \mu_l \mathbf{B} \quad P_l = \text{constant}$

Interfaces: $[[P_l + B^2 / (2\mu_0)]] = 0 \quad \mathbf{B} \cdot \mathbf{n} = 0$



MRXMHD approaches ideal MHD as $N \rightarrow \infty$



[1] G. Dennis et al., *Phys. Plasmas* **20**, 032509 (2013).

Stepped Pressure Equilibrium Code, SPEC

[Hudson et al Phys. Plasmas 19, 112502 (2012)]

Hudson

Vector potential is discretised using mixed Fourier & finite elements

- Coordinates (s, ϑ, ζ)
- Interface geometry $R_i = \sum_{l,m,n} R_{lmn} \cos(m\vartheta - n\zeta)$, $Z_i = \sum_{l,m,n} Z_{lmn} \sin(m\vartheta - n\zeta)$
- Exploit gauge freedom $\mathbf{A} = A_\vartheta(s, \vartheta, \zeta) \nabla \vartheta + A_\zeta(s, \vartheta, \zeta) \nabla \zeta$
- Fourier $A_\vartheta = \sum_{m,n} \alpha(s) \cos(m\vartheta - n\zeta)$
- Finite-element $a_\vartheta(s) = \sum_i a_{\vartheta,i}(s) \rho(s)$

& inserted into constrained-energy functional $F = \sum_{l=1}^N (W_l - \mu_l H_l / 2)$

- Derivatives wrt \mathbf{A} give Beltrami field $\nabla \times \mathbf{B} = \mu \mathbf{B}$
- Field in each annulus computed independently, distributed across multiple cpu's
- Field in each annulus depends on enclosed toroidal flux, poloidal flux, interfaces ξ

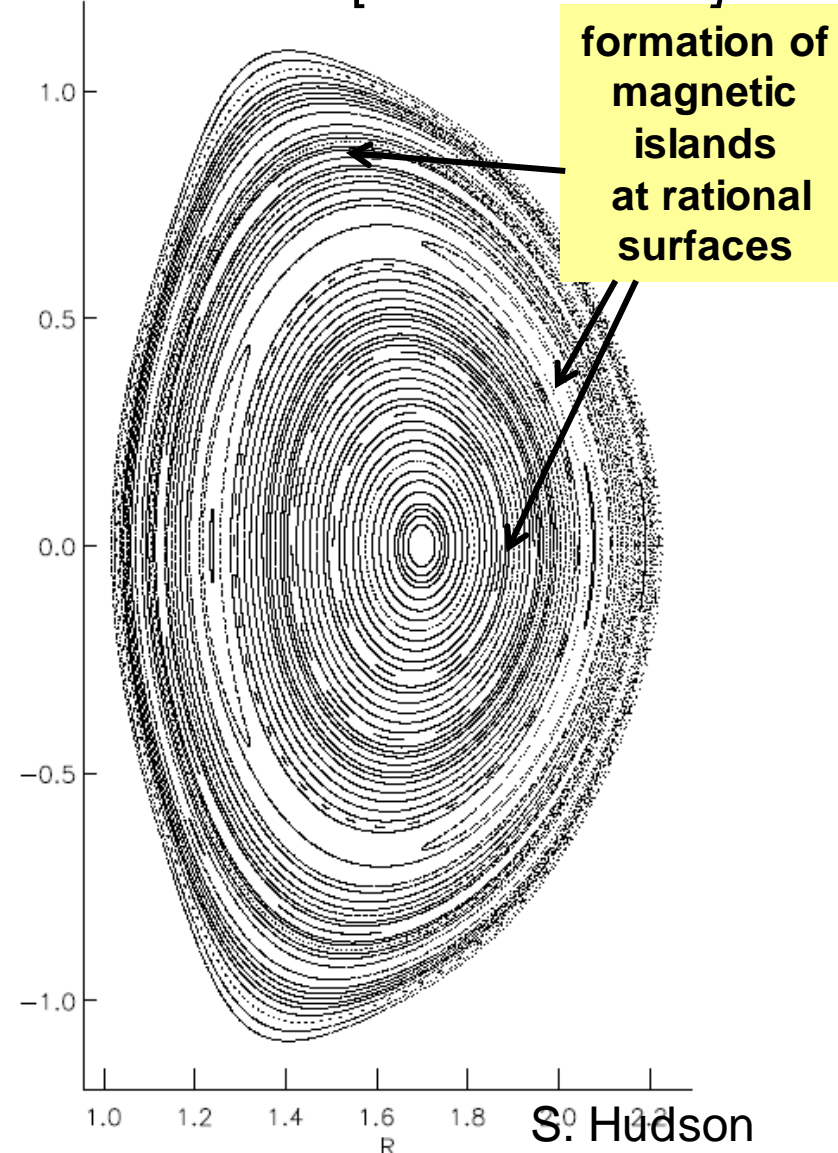
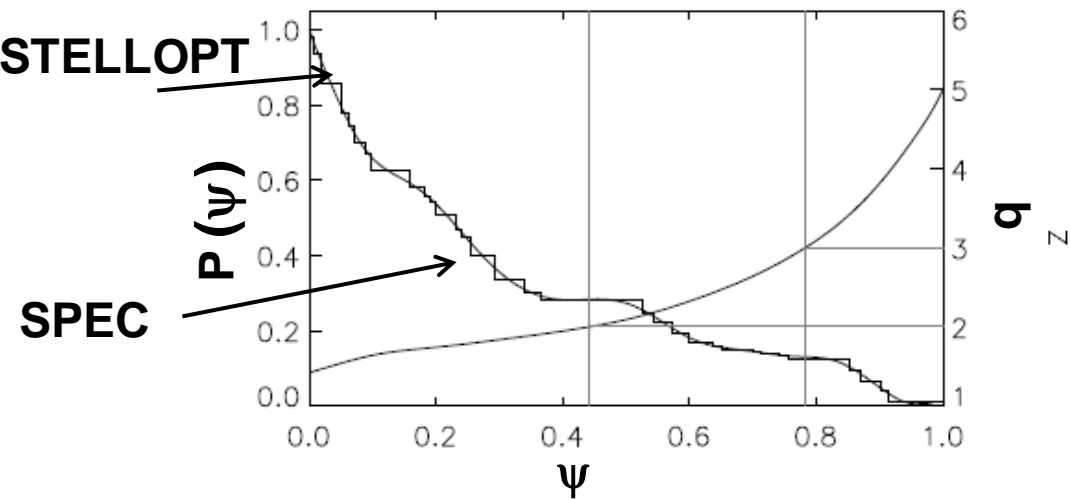
Force balance solved using multi-dimensional Newton method

- Interface geometry adjusted to satisfy force balance $\mathbf{F}[\xi] = \{ \llbracket p + B^2 / 2 \rrbracket_{m,n} \} = 0$
- Angle freedom constrained by spectral condensation,
- Derivative matrix $\nabla F[\xi]$ computed in parallel using finite difference

Example: DIID with $n=3$ applied error field

[Hudson et al Phys. Plasmas 19, 112502 (2012)]

- 3D boundary, p , q -profile from STELLOPT reconstruction [Sam Lazerson]
- Irrational interfaces chosen to coincide with pressure gradients.

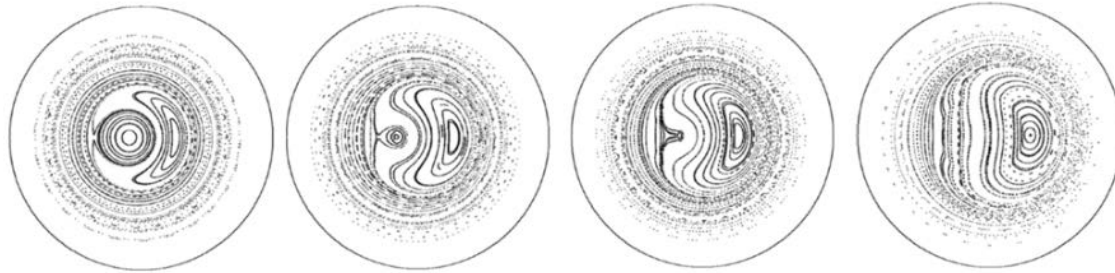


- Island formation is permitted
- No rational “shielding currents” included in calculation.

Spontaneously formed helical states

Dennis, Hudson, Terranova, Dewar, Hole

- The quasi-single helicity state is a stable helical state in RFP: becomes purer as current is increase



Double-Helical
Axis state

Increasing current

Single Helical
Axis state

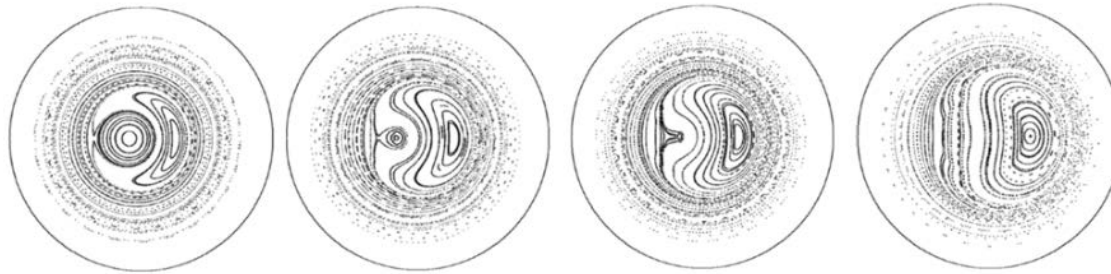
“Experimental” Poincaré plot

[Fig. 6 of P. Martin et al., Nuclear Fusion 49, 104019 (2009)]

Spontaneously formed helical states

Dennis, Hudson, Terranova, Dewar, Hole

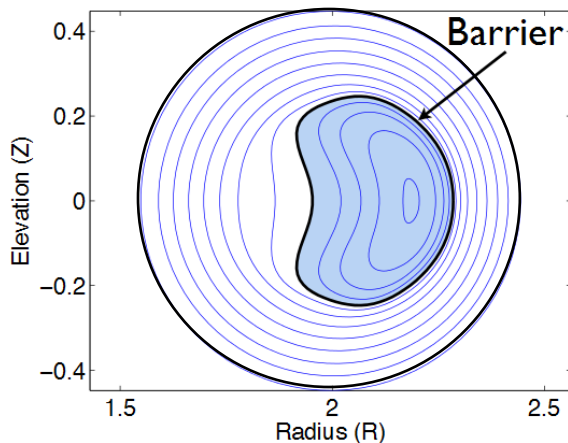
- The quasi-single helicity state is a stable helical state in RFP: becomes purer as current is increase



“Experimental” Poincaré plot

[Fig. 6 of P. Martin et al., Nuclear Fusion 49, 104019 (2009)]

Double-Helical Axis state $\xrightarrow{\text{Increasing current}}$ Single Helical Axis state

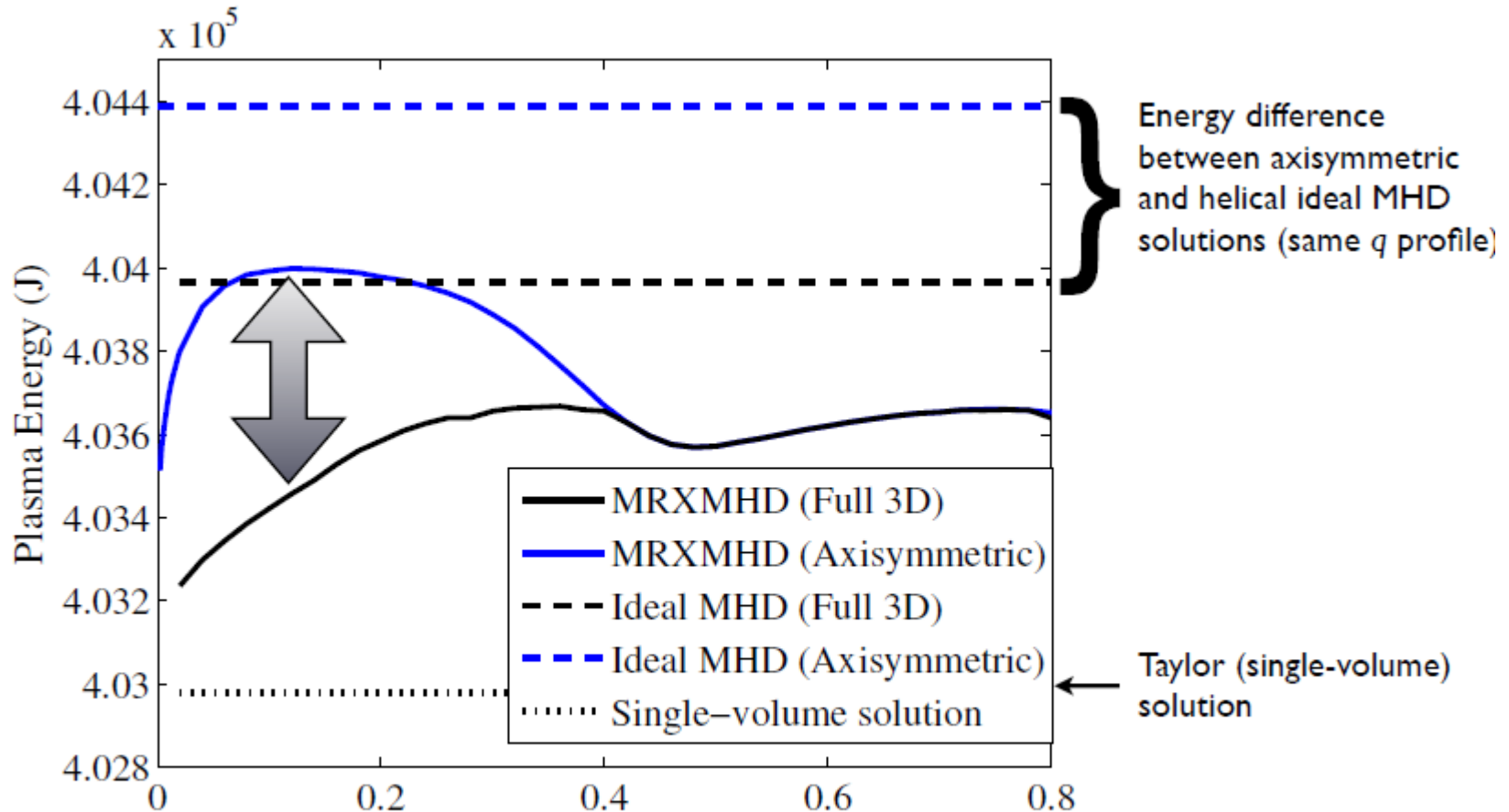


- Ideal MHD with assumed nested flux surfaces can **not** model the DAX state
- Might MRXMHD with 2 barriers offer a minimal description to describe DAX and SHAX states in the RFP?
- Model RFX-mod QSH state by a 2-interface minimum energy MRXMHD state.

[G. R. Dennis *et al* , Phys. Rev. Lett. **111**, 055003, 2013]

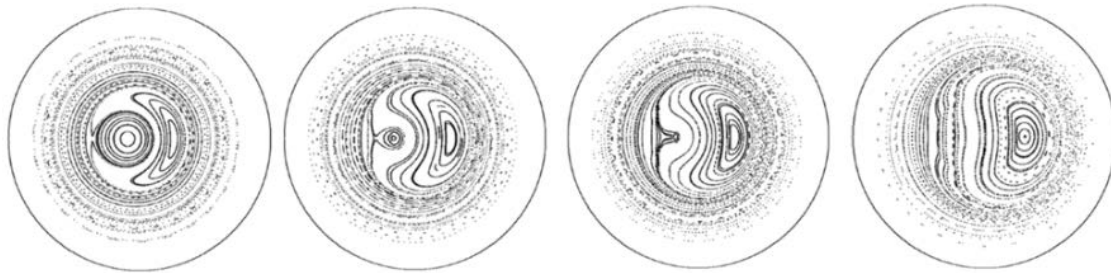
Plasma is a minimum energy state

- RFP bifurcated state has lower energy (preferred) than comparable axis-symmetric state



Ideal MHD flux surface chosen as ideal barrier

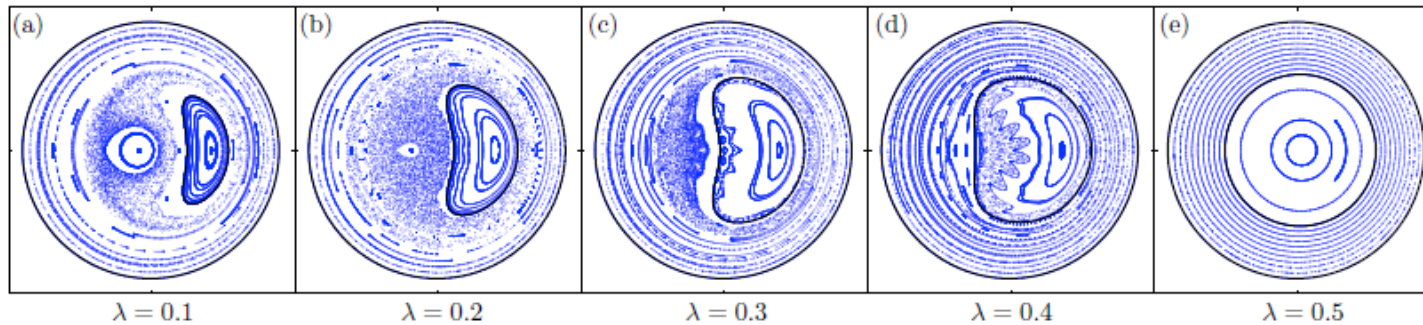
Spontaneously formed helical states



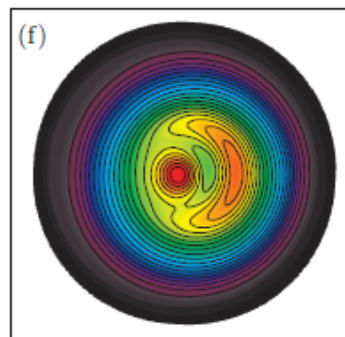
“Experimental” Poincaré plot

[Fig. 6 of P. Martin et al., Nuclear Fusion 49, 104019 (2009)]

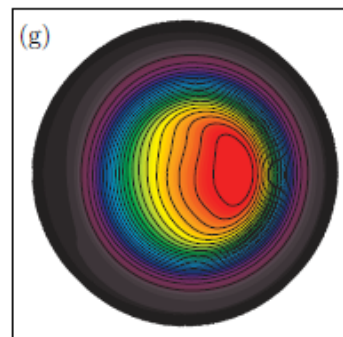
Double-Helical Axis state \longrightarrow Single Helical Axis state



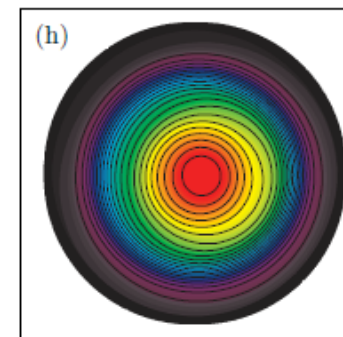
MRXMHD
Poincaré plot
G. R. Dennis
PRL



DAx state



SHAx state

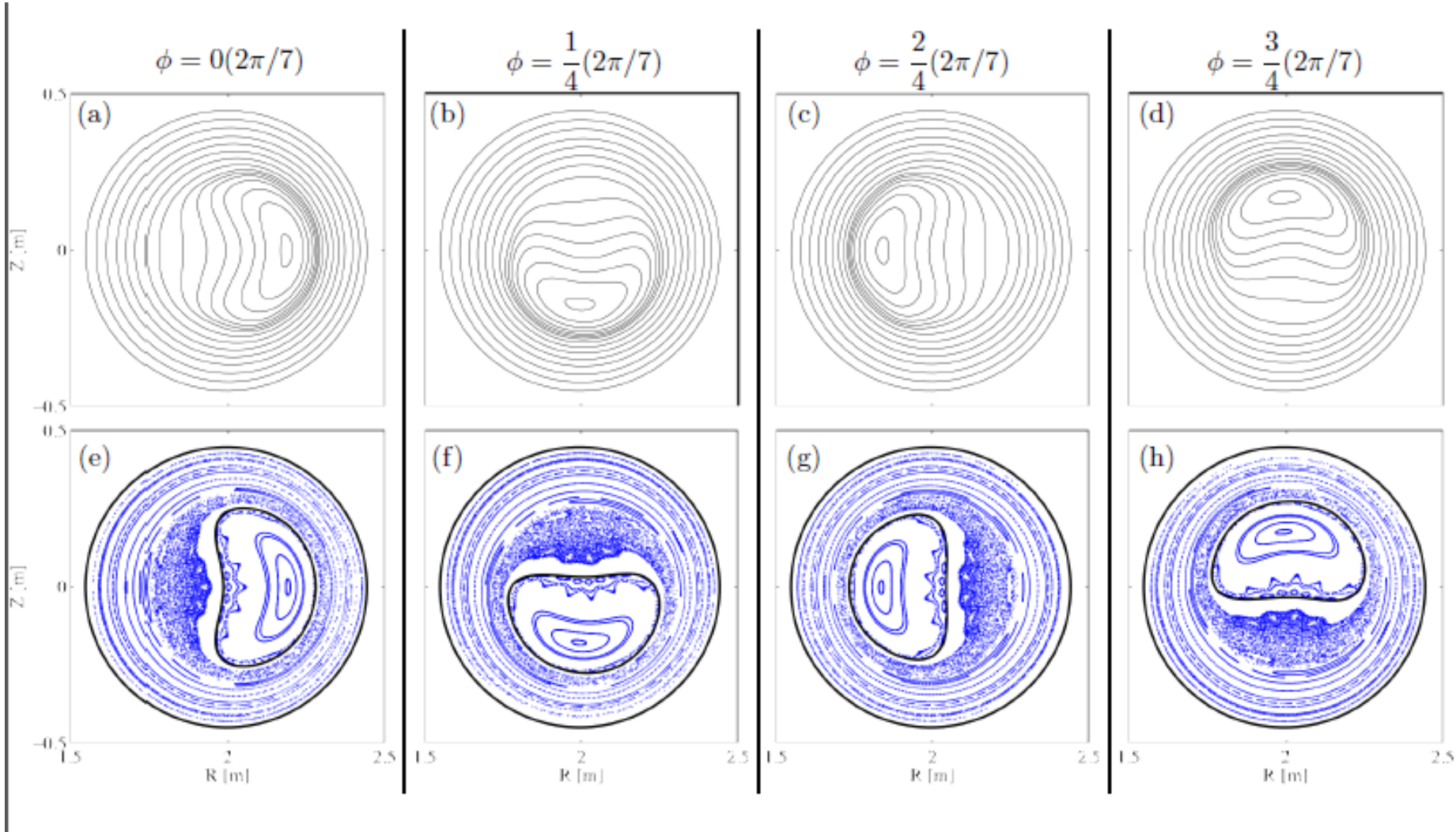


Axisymmetric
multiple-helicity state

Soft X-ray data

VMEC / SPEC comparison reveals chaos

Different toroidal cross-sections at $\lambda = 0.4$



Recent progress in MRxMHD

- Extended MRxMHD to include non-zero plasma flow
[G.R. Dennis, S.R. Hudson, R.L. Dewar, M.J. Hole, sub. Phys Plas. 15/01/2014]
- Generalized straight field line coordinates concept to fully 3D plasmas
[R. L. Dewar, S. R. Hudson, A. Gibson, *Plasma Phys. Control. Fusion*, **55**, 014004, 2013]
- Related helical bifurcation of a Taylor relaxed state to a tearing mode
[Z. Yoshida and R. L. Dewar, *J. Phys. A: Math. Theor.* **45**, 365502, 2012]
- Related ghost surfaces and isotherms in chaotic fields
[S. R. Hudson and J. Breslau, *Phys. Rev. Lett.*, **100**, 095001, 2008]
- Developed techniques to establish pressure jump a surface can support.
[M. McGann, ANU PhD thesis, 2013]

Recent progress in MRxMHD

- Computed the high- n stability of a pressure discontinuity in a 3D plasma.

[D. Barmaz, ANU Masters Thesis 2011]

- Developed “plasmoids”, representing partial magnetic island chains

[R. L. Dewar *et al*, Phys. Plas. **20**, 0832901, 2013.]

Conclusions

Anisotropy

- Extended EFIT++ to include anisotropy and flow
- Code benchmarked to Extended Soloviev
- Demonstrated strong dependence of J_ϕ with anisotropy
- Extended HELENA to include anisotropy: examined components of J_ϕ and variation of p with flux surfaces
- Developed new single adiabatic stability model, incompressible stability treatment and stability code.

MRxMHD

- Introduced/ motivated multi-region relaxed MHD, and SPEC 3D MHD code
- Described helical axis RFP with 2-interface MRXMHD model
- Summarised recent developments and directions

Constraining the flux functions to transport codes or experiment

$$\{F(\psi), \Omega(\psi), H(\psi), T_{\parallel}(\psi), \theta(\psi)\}$$

- TRANSP computes $f(E, \lambda)$: Moments give p_{\perp} , p_{\parallel} , u_{\parallel} ,
- Dependency of flux functions on (R,Z) mesh

$$T_{\parallel}(R_i, Z_i) = \frac{p_{\parallel}(R_i, Z_i)}{\left(\frac{k}{m}\right)\rho(R_i, Z_i)}$$

$$F(R_i, Z_i) = R_i B_{\phi}(R_i, Z_i) [1 - \Delta(R_i, Z_i)]$$

$$\Omega(R_i, Z_i) = \frac{v_{\phi}(R_i, Z_i)}{R_i}$$

$$H(R_i, Z_i) = \frac{p_{\parallel}(R_i, Z_i)}{\rho(R_i, Z_i)} \ln \left(\frac{\rho(R_i, Z_i) p_{\parallel}(R_i, Z_i)}{\rho_0 p_{\perp}(R_i, Z_i)} \right) - \frac{v_{\phi}^2(R_i, Z_i)}{2}$$

$$\theta(R_i, Z_i) = \frac{\left(\frac{k}{m}\right)\rho(R_i, Z_i) B(R_i, Z_i)}{p_{\parallel}(R_i, Z_i)} - \frac{\left(\frac{k}{m}\right)\rho(R_i, Z_i) B(R_i, Z_i)}{p_{\perp}(R_i, Z_i)}$$

Analytic extension to Soloviev

A. G-S Soloviev solution

$$\bar{\psi} = \left[x - \frac{1}{2}\epsilon(1 - x^2) \right]^2 + \left(1 - \frac{1}{4}\epsilon^2 \right) [1 + \epsilon\tau x(2 + \epsilon x)] \left(\frac{y}{\sigma} \right)^2$$

$$\psi = \left(\frac{a^2 B_0}{\alpha} \right) \bar{\psi}$$

$$R = ax + R_0$$

$$Z = ay$$

$$p_S(\bar{\psi}) = p'[1 - \bar{\psi}]$$

$$F_S^2(\bar{\psi}) = F'^2[1 - \bar{\psi}] + R_0^2 B_0^2$$

Analytic extension to Soloviev

A. G-S Soloviev solution

$$\bar{\psi} = \left[x - \frac{1}{2}\epsilon(1-x^2) \right]^2 + \left(1 - \frac{1}{4}\epsilon^2 \right) [1 + \epsilon\tau x(2 + \epsilon x)] \left(\frac{y}{\sigma} \right)^2$$

$$\psi = \left(\frac{a^2 B_0}{\alpha} \right) \bar{\psi}$$

$$R = ax + R_0$$

$$Z = ay$$

$$p_S(\bar{\psi}) = p'[1 - \bar{\psi}]$$

$$F_S^2(\bar{\psi}) = F'^2[1 - \bar{\psi}] + R_0^2 B_0^2$$

B. G-S with flow, anisotropy

$$\begin{aligned} p_{\perp} &= p_{\perp}(R, B, \psi) \\ \nabla \cdot \left[\left(\frac{\nabla \psi}{R^2} \right) \right] - \frac{F^2}{(1-\Delta)^2} \nabla_{\psi} \log(1-\Delta) &= \\ -\frac{1}{(1-\Delta)} \left(\frac{\partial p_{\perp}}{\partial \psi} \right)_{B,R} - \frac{F(\psi)F'(\psi)}{R^2(1-\Delta)^2} &= \\ \left(\frac{\partial p_{\perp}}{\partial R} \right)_{\psi,B} &= \rho R \Omega(\psi)^2 \\ \left(\frac{\partial p_{\perp}}{\partial B} \right)_{\psi,R} &= -\Delta B \end{aligned} \quad \left. \vphantom{\begin{aligned} p_{\perp} &= p_{\perp}(R, B, \psi) \\ \nabla \cdot \left[\left(\frac{\nabla \psi}{R^2} \right) \right] - \frac{F^2}{(1-\Delta)^2} \nabla_{\psi} \log(1-\Delta) &= \\ -\frac{1}{(1-\Delta)} \left(\frac{\partial p_{\perp}}{\partial \psi} \right)_{B,R} - \frac{F(\psi)F'(\psi)}{R^2(1-\Delta)^2} &= \\ \left(\frac{\partial p_{\perp}}{\partial R} \right)_{\psi,B} &= \rho R \Omega(\psi)^2 \\ \left(\frac{\partial p_{\perp}}{\partial B} \right)_{\psi,R} &= -\Delta B \end{aligned}} \right\} \quad (\#)$$

To maintain same ψ geometry as A keep $p_{\perp}'(\psi)$ and $F'(\psi)$ same, while satisfying (#). Choose

$$p_{\perp}(R, B, \psi) = \frac{1}{2}\rho_0\Omega_0^2 R^2 - \frac{\Delta_0}{2} B^2 + \sigma_0 p_S(\psi)$$

$$p_{\parallel}(R, B, \psi) = \frac{1}{2}\rho_0\Omega_0^2 R^2 + \frac{\Delta_0}{2} B^2 + \sigma_0 p_S(\psi)$$

$$F^2(\psi) = \sigma_0^2 F_S^2(\psi)$$

Analytic extension to Soloviev

A. G-S Soloviev solution

$$\bar{\psi} = \left[x - \frac{1}{2}\epsilon(1-x^2) \right]^2 + \left(1 - \frac{1}{4}\epsilon^2 \right) [1 + \epsilon\tau x(2 + \epsilon x)] \left(\frac{y}{\sigma} \right)^2$$

$$\psi = \left(\frac{a^2 B_0}{\alpha} \right) \bar{\psi}$$

$$R = ax + R_0$$

$$Z = ay$$

$$p_S(\bar{\psi}) = p'[1 - \bar{\psi}]$$

$$F_S^2(\bar{\psi}) = F'^2[1 - \bar{\psi}] + R_0^2 B_0^2$$

- Solution exhibits de-coupling of magnetic and pressure surfaces, *but* functional dependence of pressure in analytical solution unrealistic because of lack of transport physics i.e. $p_{\perp}(\rho, B, \psi) / \rho \neq T_{\perp}(B, \psi)$, as in EFIT TENSOR.

B. G-S with flow, anisotropy

$$\begin{aligned} p_{\perp} &= p_{\perp}(R, B, \psi) \\ \nabla \cdot \left[\left(\frac{\nabla \psi}{R^2} \right) \right] - \frac{F^2}{(1-\Delta)^2} \nabla_{\psi} \log(1-\Delta) &= \\ -\frac{1}{(1-\Delta)} \left(\frac{\partial p_{\perp}}{\partial \psi} \right)_{B,R} - \frac{F(\psi)F'(\psi)}{R^2(1-\Delta)^2} &= \\ \left(\frac{\partial p_{\perp}}{\partial R} \right)_{\psi,B} &= \rho R \Omega(\psi)^2 \\ \left(\frac{\partial p_{\perp}}{\partial B} \right)_{\psi,R} &= -\Delta B \end{aligned} \quad \left. \vphantom{\begin{aligned} p_{\perp} &= p_{\perp}(R, B, \psi) \\ \nabla \cdot \left[\left(\frac{\nabla \psi}{R^2} \right) \right] - \frac{F^2}{(1-\Delta)^2} \nabla_{\psi} \log(1-\Delta) &= \\ -\frac{1}{(1-\Delta)} \left(\frac{\partial p_{\perp}}{\partial \psi} \right)_{B,R} - \frac{F(\psi)F'(\psi)}{R^2(1-\Delta)^2} &= \\ \left(\frac{\partial p_{\perp}}{\partial R} \right)_{\psi,B} &= \rho R \Omega(\psi)^2 \\ \left(\frac{\partial p_{\perp}}{\partial B} \right)_{\psi,R} &= -\Delta B \end{aligned}} \right\} \quad (\#)$$

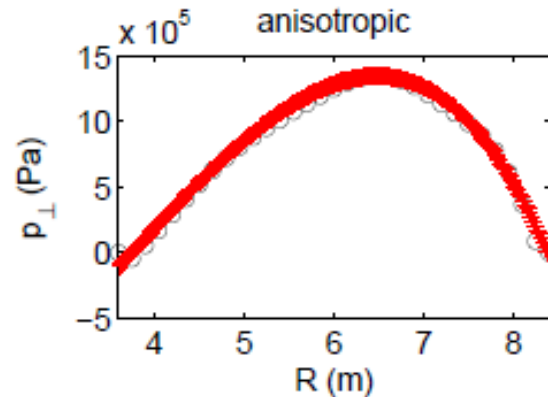
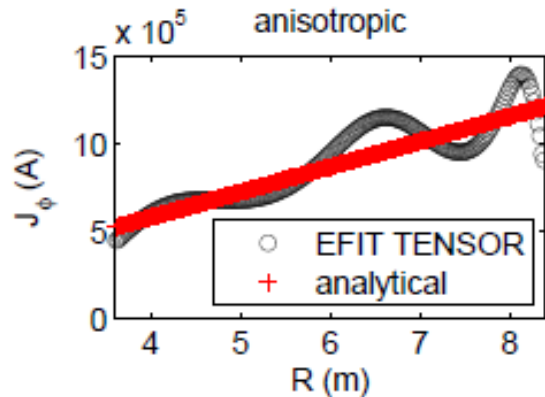
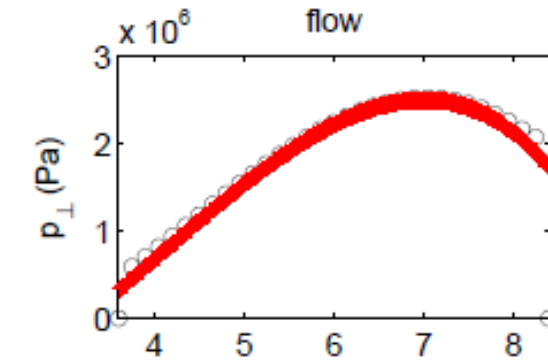
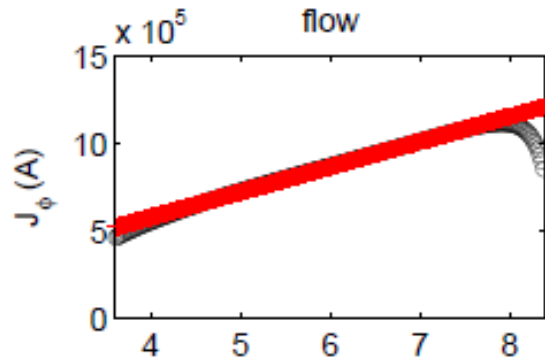
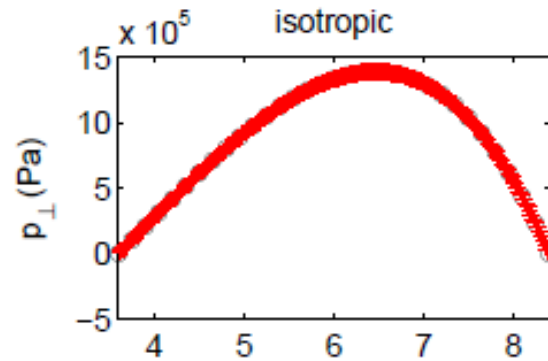
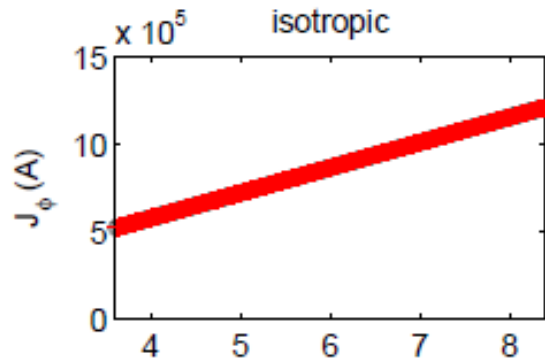
To maintain same ψ geometry as A keep $p_{\perp}'(\psi)$ and $F'(\psi)$ same, while satisfying (#). Choose

$$p_{\perp}(R, B, \psi) = \frac{1}{2} \rho_0 \Omega_0^2 R^2 - \frac{\Delta_0}{2} B^2 + \sigma_0 p_S(\psi)$$

$$p_{\parallel}(R, B, \psi) = \frac{1}{2} \rho_0 \Omega_0^2 R^2 + \frac{\Delta_0}{2} B^2 + \sigma_0 p_S(\psi)$$

$$F^2(\psi) = \sigma_0^2 F_S^2(\psi)$$

J_ϕ a strong function of anisotropy



e.g. ITER-like plasma

ϵ	0.4
σ	1
τ	1
R_0	6 m
B_0	5 T
α	-3
ρ_0	1×10^{-7}
Ω_0	0 or $7 \times 10^5 \text{ rad s}^{-1}$
Δ_0	0 or 4×10^{-3}
I_p	16 MA
q^*	1.6
β_p	1.0
β_T	0.07

$$p_\perp / p_\parallel \sim 1.06$$

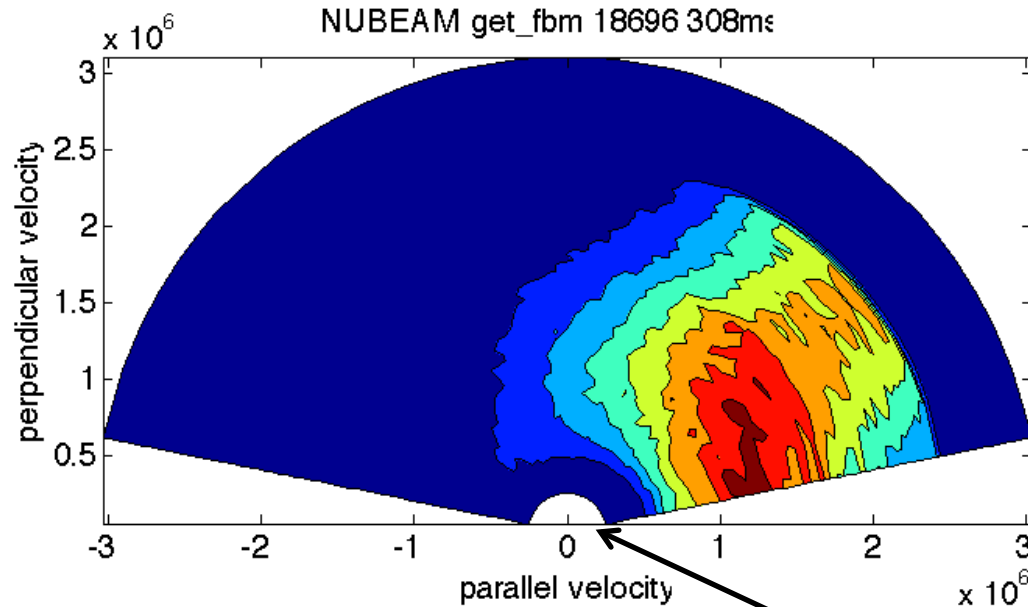
P_\perp a good match
between EFIT
TENSOR and analytic
working,

however

J_ϕ very different –
inferred magnetic
topology can be
radically different

p_{\parallel} , p_{\perp} , flow from $f(E, \lambda)$ moments

$r/a=0.25$



[35th EPS 2008; M.K.Lilley et al]

Thermal population

$$E = 0.5mv^2, \quad v_{\parallel} = v \cos \lambda$$

$$n = \int_0^{\infty} \int_{-1}^1 \hat{f}(E, \lambda) d\lambda dE$$

$$nu_{\parallel} = \int_0^{\infty} \int_{-1}^1 v_{\parallel} \hat{f}(E, \lambda) d\lambda dE$$

$$p_{\parallel} = m \int_0^{\infty} \int_{-1}^1 (v_{\parallel} - u_{\parallel})^2 \hat{f}(E, \lambda) d\lambda dE$$

$$p_{\perp} = \frac{m}{2} \int_0^{\infty} \int_{-1}^1 v_{\perp}^2 \hat{f}(E, \lambda) d\lambda dE.$$

$v_{\parallel} > v_{\perp}$ in distribution function, *however...*

p_{\parallel} computed with subtracted $u_{\parallel} \Rightarrow p_{\parallel} < p_{\perp}$

In single fluid limit, need to add thermal species and recompute moments to get complete anisotropy.

Generalised Taylor Relaxation:

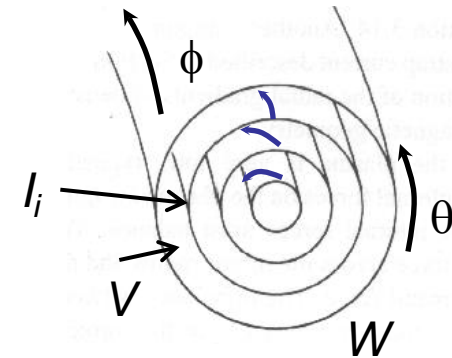
Multiple Relaxed Region MHD (MRXMHD)

R. L. Dewar

- Assume each invariant tori I_i act as ideal MHD barriers to relaxation, so that Taylor constraints are localized to subregions.

New system comprises:

- N plasma regions P_i in relaxed states.
- Regions separated by ideal MHD barrier I_i .
- Enclosed by a vacuum V ,
- Encased in a perfectly conducting wall W



$$W_i = \int_{R_i} \left(\frac{B_i^2}{2\mu_0} + \frac{P_i}{\gamma - 1} \right) d\tau^3$$

$$H_i = \int_V (\mathbf{A}_i \cdot \mathbf{B}_i) d\tau^3$$

Seek minimum energy state:

$$F = \sum_{l=1}^N (W_l - \mu_l H_l / 2)$$

$$P_l : \quad \nabla \times \mathbf{B} = \mu_l \mathbf{B}$$

$$P_l = \text{constant}$$

$$I_l : \quad \mathbf{B} \cdot \mathbf{n} = 0$$

$$[[P_l + B^2 / (2\mu_0)]] = 0$$

$$V : \quad \nabla \times \mathbf{B} = 0$$

$$\nabla \cdot \mathbf{B} = 0$$

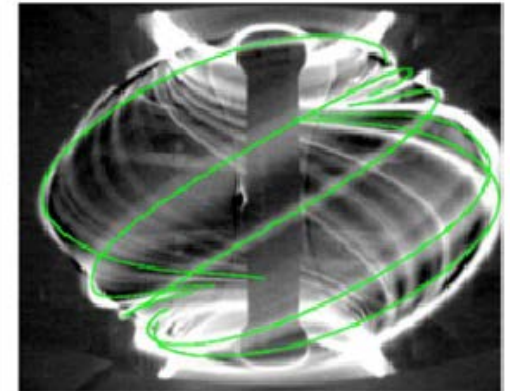
$$W : \quad \mathbf{B} \cdot \mathbf{n} = 0$$

Ongoing work/ plans for MRxMHD (1)

- Free-boundary extension: including vacuum region and external conductors

Enables calculation of stability to external modes and response due to Resonant Magnetic Perturbation (RMP) coils – designed to kill Edge Localised Modes (ELMs)

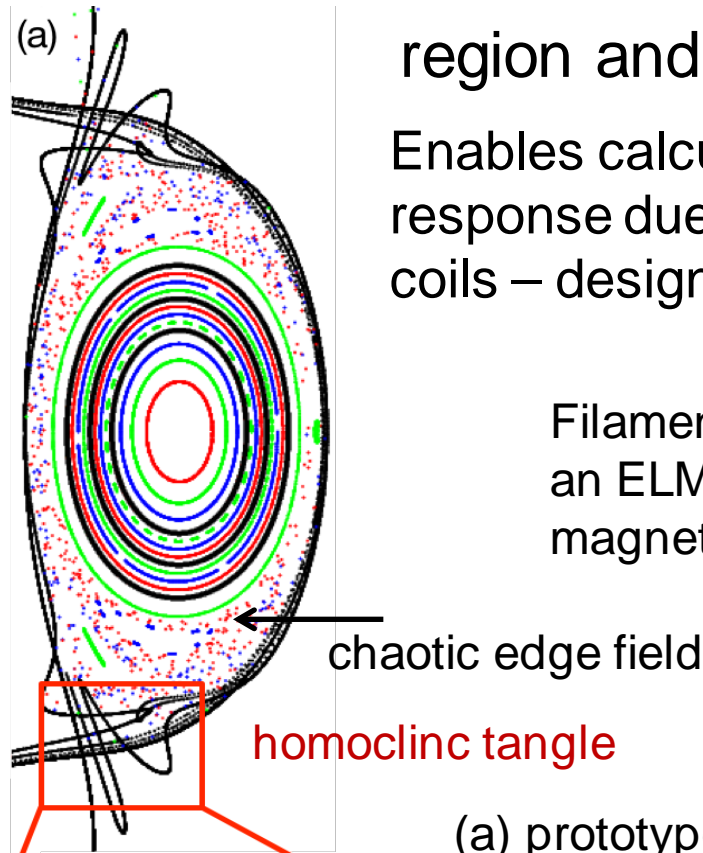
Filamentary structures during an ELM in MAST with the magnetic field lines overlaid.



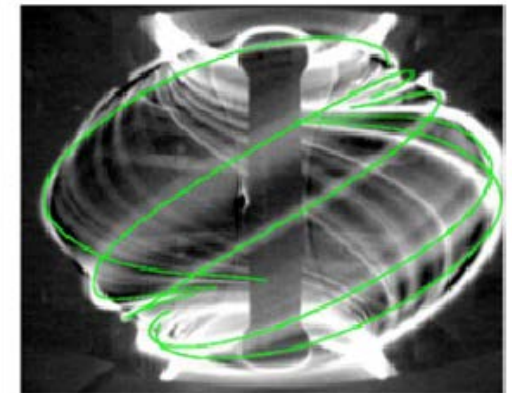
Ongoing work/ plans for MRxMHD (1)

- Free-boundary extension: including vacuum region and external conductors

Enables calculation of stability to external modes and response due to Resonant Magnetic Perturbation (RMP) coils – designed to kill Edge Localised Modes (ELMs)

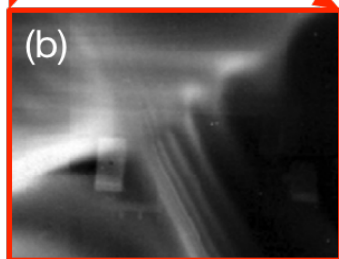


Filamentary structures during an ELM in MAST with the magnetic field lines overlaid.



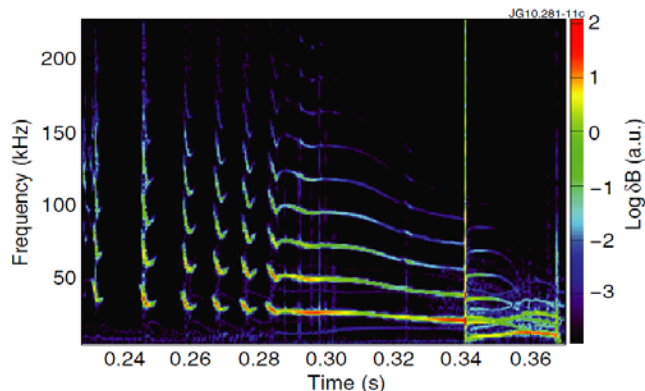
(a) prototype calculation by S. Hudson performed for an illustrative cross-section with a large perturbation

(b) lobe structure observed in MAST in divertor target region during RMP.



Ongoing work/ plans for MRxMHD (2)

- Each region is relaxed, but boundary interfaces can be unstable to island formation, and support pressure jumps, currents:
 - Determine interface disruption-limit by island formation
 - Global stability of MRxMHD equilibria – determine stability to formation of islands and chaotic fields.
 - Impact of flow-shear on ELMs stability in RMP modified plasmas.
- Explanation of helical states exist in tokamaks form an energy principle: islands, “long-lived” modes, sawteeth



Fishbone oscillations (bursty, up to 0.28s) that initiate a long-living $n = 1$ kink mode (at frequency 30 kHz) in MAST discharge #16038.

Single-adiabatic model

- Extending the MHD model to anisotropy
 - isotropic perturbed pressure \tilde{p} and assuming zero net heat flow. The perturbation \tilde{p} is isotropic

$$\vec{P}_0 + \vec{P}_1 = p_{\perp} \mathbf{I} + (p_{\parallel} - p_{\perp}) \mathbf{b}\mathbf{b} + \tilde{p} \mathbf{I} =$$

$$\begin{pmatrix} p_{\perp} + \tilde{p} & 0 & 0 \\ 0 & p_{\perp} + \tilde{p} & 0 \\ 0 & 0 & p_{\parallel} + \tilde{p} \end{pmatrix} \quad \backslash \quad \begin{aligned} \vec{P} &\rightarrow \tilde{p} \mathbf{I} + \tilde{\pi} \\ \text{Tr } \nabla \cdot \vec{Q} &\rightarrow 0 \\ \text{Tr } \tilde{\pi} &\rightarrow 0 \end{aligned}$$

Assumes zero net heat flow

Generalizing to Anisotropic plasma (non-compressional)

- The Lagrangian perturbed distribution function is zero

$$f_{bounce} \ll f_{mode} \rightarrow CGL$$

$$\tilde{f} = -\xi_{\perp} \cdot \nabla F - \frac{\partial F}{\partial \varepsilon} \left(\frac{1}{i\omega} \frac{M}{e} E_{\parallel} + v_{\parallel}^2 \xi_{\perp} \cdot \kappa - \mu B \xi_{\perp} \cdot \kappa - \mu B \nabla \cdot \xi_{\perp} \right)_{bounce}$$

- The fluid closure equations are ^{Note for Matthew: this equation has}

$$p_{\parallel 1} = -\xi_n \left[\frac{\partial p_{\parallel}}{\partial n} - (p_{\parallel} - p_{\perp}) \frac{\partial \ln B}{\partial n} \right]$$

$$p_{\perp 1} = -\xi_n \left[\frac{\partial p_{\perp}}{\partial n} - (2p_{\perp} + \hat{c}) \frac{\partial \ln B}{\partial n} \right]$$

- magnetic drift effect (only EXB drift)
 - non-local resonance and Landau damping
 - FOW and FLR effects
- otherwise you need more complicated closures

$$\hat{c} \equiv \sum_s M_s \int \frac{B}{v_{\parallel}} (\mu B)^2 \frac{\partial F_s}{\partial \varepsilon} d\mu d\varepsilon$$

Impact of anisotropy & flow on stability

- MHD cannot deal with anisotropy
 - MHD pressure is isotropic: , p_{\parallel} and p_{\perp} are combined into a single scalar pressure $P = \frac{1}{2}(p_{\parallel} + p_{\perp})$. $\frac{d}{dt} \left(\frac{p}{\rho^{5/3}} \right) = 0$
 - × Parallel heat flow is extreme due to streaming particles
 - × Kinetic effects are significant (Landau damping)
- Use a fluid model as a first approximation:
 - **New** Single adiabatic (SA) model extension to MHD
 - Double-adiabatic (CGL)
 - Collisionless, p_{\parallel} and p_{\perp} doing **independent** work
 - No streaming particle heat flow
 - Does not reduce to MHD in the isotropic limit
 - Double-polytropic law
 - Extension of CGL but not physically solid
 - Going to higher order moments and truncate at arbitrary order

$$\frac{d}{dt} \left(\frac{p_{\perp}}{\rho B} \right) = 0,$$

$$\frac{d}{dt} \left(\frac{p_{\parallel} B^2}{\rho^3} \right) = 0.$$

$$\frac{d}{dt} \left(\frac{p_{\perp}}{\rho B^{\gamma_{\perp}-1}} \right) = 0$$

$$\frac{d}{dt} \left(\frac{p_{\parallel} B^{\gamma_{\parallel}-1}}{\rho^{\gamma_{\parallel}}} \right) = 0$$